Netherlands Journal of Geosciences

www.cambridge.org/njg

Review

**Cite this article:** Schaumann RM, Capperucci RM, Bungenstock F, McCann T, Enters D, Wehrmann A, and Bartholomä A. The Middle Pleistocene to early Holocene subsurface geology of the Norderney tidal basin: new insights from core data and high-resolution sub-bottom profiling (Central Wadden Sea, southern North Sea). *Netherlands Journal of Geosciences*, Volume 100, e15. https://doi.org/10.1017/njg.2021.3

Received: 8 July 2020
Revised: 29 January 2021
Accepted: 1 February 2021

**Keywords:**
Main Drenthe; fine gravel analysis; Eemian; tidal inlet; sedimentary facies

**Author for correspondence:**
Robin M. Schaumann,
Email: robin.schaumann@uni-bonn.de



CAMBRIDGE UNIVERSITY PRESS

# The Middle Pleistocene to early Holocene subsurface geology of the Norderney tidal basin: new insights from core data and high-resolution sub-bottom profiling (Central Wadden Sea, southern North Sea)

Robin M. Schaumann[1,2], Ruggero M. Capperucci[2], Friederike Bungenstock[3], Tom McCann[1], Dirk Enters[3], Achim Wehrmann[2] and Alexander Bartholomä[2]

[1]Institute of Geosciences, University of Bonn, Nussallee 8, 53115 Bonn, Germany; [2]Senckenberg am Meer, Marine Research Department, Südstrand 40, 26382 Wilhelmshaven, Germany and [3]Lower Saxony Institute for Historical Coastal Research, Viktoriastraße 26–28, 26382 Wilhelmshaven, Germany

**Abstract**

Pleistocene strata of the Wadden Sea region are mostly covered by an up to 10 m thick sediment wedge deposited during the Holocene transgression. However, tidal inlets cut deep into the Holocene succession, causing Middle Pleistocene to early Holocene glacial and interglacial deposits to outcrop at the channel bottom. To investigate how the lithological properties and/or morphologies of these deposits affect the development of Holocene tidal inlets (e.g. limiting erosional processes), we analysed a series of eight cores to verify three high-resolution sub-bottom transects – and thus – to extend point-based data over a broader area. Furthermore, eight additional new cores (16 WASA cores in total), and 14 reinterpreted cores from the LBEG (Geological Survey of Lower Saxony) log database, were correlated to generate three short cross-sections at the transition from the tidal inlet (Riffgat channel) to the island of Norderney, revealing a number of new aspects for the reconstruction of the Pleistocene palaeoenvironments, i.e. the last two glacials (Saalian and Weichselian) and interglacials (Holsteinian? and Eemian). A succession of Middle Pleistocene lacustrine delta deposits, belonging either to the Holsteinian or the Dömnitz temperate stage, suggests the presence of Elsterian tunnel valleys located below the island. Furthermore, we verified the presence of an Eemian mixed tidal-flat system overlain by an Eemian sand tidal flat below the western head of Norderney which is, in contrast to suggestions from previous studies, not fully eroded in this area. Finally, we demonstrate that the Saalian moraine (Drenthe Main Till) functions as a limiting constraint in the vertical development of the Holocene/modern Riffgat channel. Our results provide a better understanding of the Quaternary stratigraphy of the central Wadden Sea as well as the influence of the subsurface geology on the architecture and evolution of tidal channels.

## Introduction

The present shape of the coastline of the southern North Sea is the result of the interaction of various factors, for example, the glacial/periglacial Weichselian conditions (e.g. coversands, fluvial drainage systems) and deposits, the reorganisation of these conditions during the Holocene transgression, and – since the 9th century AD – coastal engineering (terps, land reclamation, diking) (Behre, 2004, 2007; Streif, 2004; Vink et al., 2007; Vos & Knol, 2015; Vos et al., 2020). The reconstruction of the Quaternary evolution of this coastal zone is mainly based on core data from a variety of approaches (coastal engineering, hydrology, resources, research), which results in large data sets providing among others litho-, bio- and chronostratigraphic data and palaeoenvironmental, palaeoecological and sedimentological interpretations (for a review of the Dutch Wadden Sea data sets see Pierik & Cohen, 2020; for Lower Saxony data sets see NIBIS® Kartenserver 2020a–c).

The existing palaeoenvironmental reconstructions of NW Germany have mainly focused on the Holocene. Vos & Knol (2015) and Karle et al. (2021) presented a comprehensive compilation of these results. To date, research on the Pleistocene deposits has mainly concentrated on the reconstruction of the locations of the ice margins for glacial periods, or coastlines for interglacials (e.g. Streif, 2004; Ehlers et al., 2011). The reconstruction of Pleistocene surfaces, however, has been largely neglected as few reliable data are available. As a consequence, the presence of Eemian deposits in the study area is still unclear. According to Dechend (1950, 1952, 1954, 1958), these deposits are present, but according to Sindowski (1973) and Streif (1990) they are not.

Within the frame of the joint WASA project (The Wadden Sea as an archive of landscape evolution, climate change and settlement history; Bittmann et al., 2021) this study was initiated in order to reconstruct the regional Holocene coastal evolution in the light of environmental changes controlled by climate, local hydrology and sedimentary processes. An interdisciplinary data set, including hydroacoustic profiles, sediment cores and multi-proxy data (e.g. radiocarbon dating, marine micro- and macrofauna ecology, pollen analysis) was generated and analysed, in order to examine both the chronology and environmental changes, which occurred across the region within the determined time frame. To extend the detailed information inferred from point-based data sets (e.g. cores) to a broader area, we followed an integrated approach using hydroacoustic data (e.g. Wunderlich & Müller, 2003) to reduce the coarsening effect due to interpolation between points (cores). This is particularly true in the case of small-scale articulated stratigraphic sequences and palaeomorphologies, where the interpolation among point-based data can omit the local variability. In addition, the ability to resolve and describe the local stratigraphy at high resolution is an essential requirement for palaeoclimatological studies (e.g. Eriş et al., 2011; Novak et al., 2017) as it allows the evolution of sedimentary successions to be deciphered also in settings with low sedimentation rates and/or significant erosion or non-deposition.

Several authors have demonstrated that hydroacoustic data, and more specifically shallow sub-bottom profiling, can be successfully used to identify and describe glacial and interglacial deposits (e.g. Grant & Schreiber, 1990; Bart & Anderson, 1997; Wunderlich & Müller, 2003; Bart & Santis, 2012; Lindeque et al., 2016; Saleh & Rabah, 2016) due to their contrasting lithologies. This is an essential requirement for the reconstruction of the Pleistocene/Holocene succession, for example, in the southern Baltic Sea (Gelumbauskaitė, 2000; Niedermeyer et al., 2002). Ottesen et al. (2014), Buckley (2017), Lamb et al. (2017) and Coughlan et al. (2018) have already applied this technique to North Sea data sets, although mainly in studies of offshore areas.

The tidal inlets are considered to be highly dynamic systems mainly controlled by tidal prism and geological factors (FitzGerald, 2015). As they cut deep into the Holocene coastal sediment wedge, they may expose the underlying Pleistocene or older strata. The analysis and understanding of the entire stratigraphic succession is essential when estimating the effect of Pleistocene deposits and/or morphologies on the evolution of Holocene tidal channel systems. Up to now there have been no extensive investigations for this time interval (Pleistocene/Holocene) in the tidal inlets of the German Wadden Sea.

The main aim of this study is to analyse the Middle Pleistocene to early Holocene subsurface geology in the deepest part of the Norderney tidal basin using an interdisciplinary approach and a broad range of data sets. Additionally, we want to combine point-based core log data and high-resolution sub-bottom profiler transects (Fig. 1) to reconstruct on a broader scale the influence of glacial and interglacial depositional processes on the coastal development of the East Frisian coast, and, in particular, the spatial transition from the tidal inlet to the island of Norderney, namely the Riffgat channel. For the core database we have designed a sediment facies catalogue for the Pleistocene/Holocene depositional palaeoenvironments.

## Geological setting

The North Sea is a marginal sea and forms part of the NW European shelf. The Quaternary-age geological history of the North Sea Basin was mainly influenced by the processes associated with glaciation, which resulted in the deposition of a thick sedimentary succession including a variety of glacial, periglacial, fluvial and marine deposits (Phillips et al., 2017). During glacial phases, ice masses extended from Scandinavia and Great Britain across Northern Germany (Ehlers et al., 2011), while the interglacial phases were characterised by sea-level rise and related transgressive depositional conditions (Streif, 2004). During the last glaciation (Weichselian) the sea level dropped to 130 m below the current sea level. A marked rise in eustatic sea level followed the Last Glacial Maximum (LGM) at ~11.7 ka BP and was related to the melting of the Fennoscandian and Laurentide ice sheets. Eustatic sea-level rise and glacio-isostatic adjustment induced a shift of the shoreline of almost 600 km to the south (e.g. Kiden et al., 2002; Streif, 2004; Vink et al., 2007; Hijma & Cohen, 2010). At around 6–7 ka BP, when the North Sea reached the position of the present-day coastal area (e.g. Streif, 2004; Flemming, 2012), Holocene peat deposits and siliciclastic sediments accumulated on top of the Pleistocene sands, reaching thicknesses of up to 25 m (Streif, 2004). Changes of the ratio of accommodation space and sediment supply led to the formation of prograding swamps, resulting in peat layers intercalated in the shallow subtidal to intertidal sediments of the Holocene-age succession (Streif, 2004; Bungenstock et al., 2021).

### *Glacial and interglacial history of Northern Germany*

Two Elsterian ice advances (marine isotope stage (MIS) 10, 400–320 ka BP, cf. Ehlers et al., 1984; Litt et al., 2007) have been recorded in Northern Germany, the older of which extends as far south as the low mountain range (Central Germany), while the second is of more limited extent (Stackebrandt, 2009; Murton & Murton, 2012). Tunnel valleys developed beneath the ice masses, as described by a number of authors (e.g. Ehlers & Linke, 1989; Streif, 1990; Lutz et al., 2009; Stackebrandt, 2009). In general, these tunnel valleys are 1–100 km long (average 30 km), and 1–4 km wide (some are up to 8 km). The maximum depth of substratum erosion by these tunnel valleys is between 120 and 400 m (Streif, 1990; Lutz et al., 2009; Stackebrandt, 2009).

The Holsteinian Interglacial (MIS 9, 320–310 ka BP, cf. Geyh & Müller, 2005; Litt et al., 2007) occurred between the Elsterian and the Saalian. Holsteinian marine deposits have not been found in the study area, while terrestrial lacustrine deposits have been noted in the surrounding area (Streif, 1990; Sierralta et al., 2017). Coastal conditions within the Holsteinian were quite similar to those of the Holocene, with the coast located to the north of its present-day position in the East Frisian region.

Three major ice advances have been recorded during the Saalian (MIS 8–6, 310–126 ka BP, cf. Litt et al., 2007), namely the Main Drenthe, the Younger Drenthe and the Warthe Stadium (Ehlers et al., 2011). Among them, only the Main Drenthe advance affected the area of the modern East Frisian Islands (Rappol et al., 1989; Streif, 1990; Meyer, 2005; Litt et al., 2007; Graham et al., 2011), resulting in the deposition of outwash and moraine deposits (Streif, 1990). A phase of warm, (sub-) continental climate conditions, which occurred during the Saalian, is termed the Dömnitz temperate stage (MIS 7, 227–180 ka BP, cf. Litt et al., 2007; Urban, 2007). This temperate stage was characterised by the development of lacustrine conditions across Northern Germany, and the deposition of a series of muds and peats (Urban et al., 1988; Urban, 2007; Sierralta et al., 2017).

The subsequent climatic amelioration, which characterised the onset of the Eemian (MIS 5e, 126–115 ka BP, cf. Shackleton et al.,

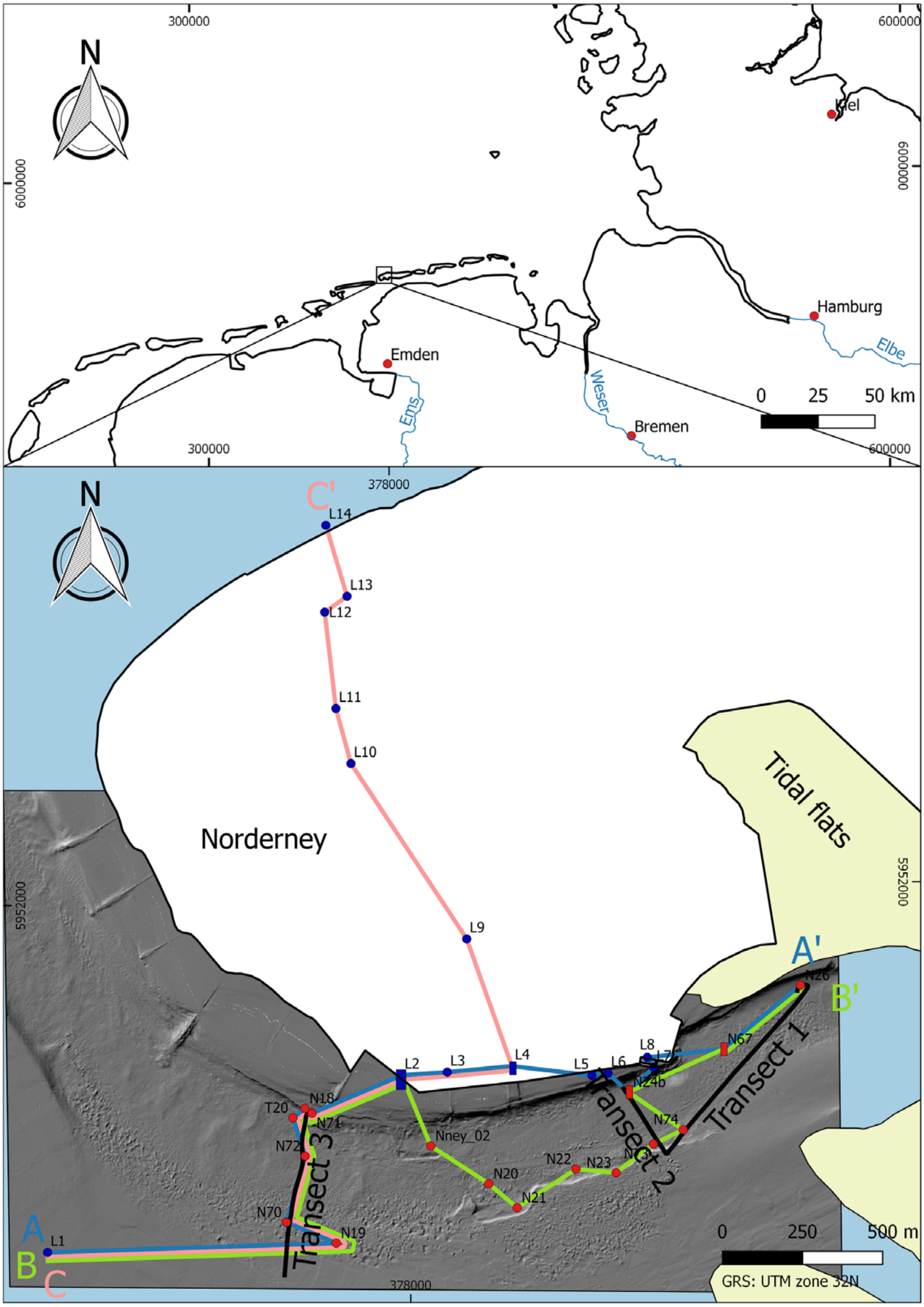


**Fig. 1.** Top: map of Northern Germany with the study area. Bottom: study area with the location of cores (red: WASA cores; blue: LBEG cores; L1 = Nordeney B13, L2 = Norderney I 26 BI Werfthalle, L3 = Norderney I 33 BVI Werfthalle, L4 = Norderney I 40 BXIII Werfthalle, L5 = Norderney 3/79 Hafen, L6 = Norderney 2/79 Hafen, L7 = Norderney 3 Hafen Fährbett, L8 = Norderney 1 Hafen Fährbett, L9 = Norderney Bohrlochreihe II. Nr. 1–2, L10 = Norderney H 51 Kinderheim Seldhausenstr., L11 = Norderney H 53 Kinderheim, L12 = Norderney H52 Kinderheim Luciusstr., L13 = Norderney B 6-1, L14 = Norderney B 7-1), sub-bottom transects and cross-sections. Data source: bathymetric data used with permission of the Lower Saxony Water Management, Coastal Defence and Nature Conservation Agency (NLWKN)

2003; Schokker et al., 2004) represents the final interglacial period of the Pleistocene (Caspers et al., 2002; Litt et al., 2007). During this period the eustatic sea-level rise resulted in a higher sea level than that of the subsequent Holocene (Turner, 2000; Streif, 2004; Ehlers et al., 2011). However, the Central Wadden Sea region was less affected by the rising sea level, due to the coeval uplift related to the ongoing glacio-isostasic adjustment. According to Sindowski (1973), Eemian-age deposits in the East Frisian region can be subdivided into three facies: marine, fluvial, and limnic to semi-terrestrial. Eemian marine deposits in the area of Norderney and the Ems Estuary were investigated in detail by Dechend (1950, 1952, 1954, 1958) and Dechend & Sindowski (1956), who noted the presence of a sandy tidal-flat system. Dechend (1950) recognised a transgressional and a regressional trend within the Eemian succession, with the average boundary (i.e. transgressional/regressional) described at a depth of −12.5 m NHN (Normalhöhennull, German standard elevation zero).

Climatic cooling marked the onset of the Weichselian (MIS 5d-2, 115,000–11,653 ± 99 a BP, cf. Behre & Lade, 1986; Serjup et al., 1994; Huijzer & Vandenberghe, 1998; Litt et al., 2007; Walker et al., 2019), a period characterised by at least four major ice advances in the Middle Weichselian (first advance = LGM) alone. These advances did not extend as far as the maximums of the previous Elsterian and Saalian glaciations, nor did they extend as far as the study area. In the region of the East Frisian Islands, the Weichselian glacial conditions resulted in the deposition of periglacial sands. These sands, which have been referred to in the literature as 'brown sands' (e.g. Sindowski, 1973; Streif, 1990), are mainly related to the deposition of continental sediments. However, according to Streif (1990), the precise stratigraphic age of these continental sediments within the Weichselian is problematic due to the predominance of periglacial structures, such as cryoturbation and ice wedges, disrupting the stratigraphy, as well as a distinct lack of interbedded interstadial sediments. Sindowski (1973) and Streif (1990) have subdivided the East Frisian Weichselian deposits into three facies, namely fluvial, flood-basin–freshwater and aeolian, based on their lithology. During the LGM the sea level dropped to 110–130 m below the present-day level (Streif, 2004). As a consequence, the coastline was located almost 600 km further north (see also Hepp et al., 2019). Subsequent climate warming resulted in a sea-level rise, causing the development of the Wadden Sea. This relative sea-level rise was essentially driven by the melting of the ice masses, glacio-isostatic adjustment, ongoing plate tectonics, sediment compaction and changing tidal influences (Streif & Köstner, 1978).

### *Norderney Island*

Norderney is part of a barrier island system within the Wadden Sea. The island is separated from the neighbouring islands by high wave-energy mesotidal inlet systems, with a mean tidal range of 2.4 m (BSH, 2020). In the western tidal inlet, the Norderneyer Riffgat channel runs along the backside of the island, parallel to its southern coastline (maximum depth: −15 m NHN) (Sindowski, 1973; Streif, 1990). The Riffgat channel deeply erodes the Pleistocene succession which underlies Norderney and, thus, exposes the stratigraphic transition from the Pleistocene to the Holocene.

Pliocene-age deposits occur at a depth of approx. −35 m NHN below Norderney (Streif, 1990). These are unconformably overlain by preserved Pleistocene deposits. To the north of this Pleistocene high, the Pleistocene relief was flattened and eroded during rising sea level, leading to the development of a ravinement (Streif, 2004). According to Flemming & Davis (1994), the elevated Pleistocene relief in the area of the modern barrier islands was partially eroded by rivers, which later were transformed into estuaries by rising sea levels around 7500 years BP. The Pleistocene high is cut by a pre-Weichselian (possible Eemian-age) palaeochannel(-system) (Norderney–Hilgenrieder Rinne, Sindowski, 1973).

On top of Pliocene deposits, the Pleistocene/Holocene sedimentary succession in the western Norderney area commences with Saalian outwash deposits, overlain by 5 m of sand and gravel representing the Saalian moraine (Main Drenthe) (Rappol et al., 1989; Streif, 1990). No Holsteinian deposits have been described or recorded, which led Sindowski (1973) and Streif (1990) to conclude that the Holsteinian transgression did not extend as far south as the region of the East Frisian Islands. For Norderney, Eemian deposits were first described by Keilhack & Wildvang (1925) noting the presence of a marine sand unit, 1–1.5 km west of the island's lighthouse, unfortunately without any depth information. They based their interpretation on macro-fossils. Eemian deposits (a peat layer at a depth of −43 to −41.9 m NHN) were also described from the 'Wasserwerk, alter Brunnen II' core, which were probably deposited in the Norderney–Hilgenrieder channel (cf. Dechend, 1952, 1954; Sindowski, 1973). Dechend (1958) identified the top of the Eemian marine deposits (based on pollen analysis, micro- and macro-fossils) in the Riffgat channel at a depth of −10.2 to −13.4 m NHN. Subsequent descriptions of Eemian deposits from Norderney by Sindowski (1973) and Streif (1990), however, suggest that they are missing from the western part of the island. Based on this, Streif (1990, 2004) concluded that there had been extensive erosion of the Eemian deposits in the Norderney region. Thus, the Saalian moraine deposits are disconformably overlain by Weichselian fluvial and aeolian sediments, at a depth of −8 m NHN (Sindowski, 1973; Streif, 1990). The Pleistocene succession is overlain by Holocene peats and tidal-flat sediments, which were subsequently covered by aeolian dunes (Sindowski, 1973; Streif, 1990).

## Methods

Within the framework of the WASA project, hydroacoustic (sub-bottom) and sediment core data were collected using two ships, RV *Senckenberg* and RV *Burchana*, from both the offshore and the back-barrier sides of Norderney Island between 2016 and 2018. In the back-barrier area, where the present study is located, three hydroacoustic transects were gathered along the Riffgat channel (Fig. 1): one central transect (broadly following the maximum depth of the channel), to investigate the lowest part of the sedimentary succession; and two lateral transects running parallel to the central one, to document the Pleistocene/Holocene transition and the Holocene development of the tidal-inlet/tidal-flat system. Several coring transects crossing the Riffgat channel were also collected. The coring locations were initially planned at the cross-points of the hydroacoustic grid. Additional locations were added later, based on the initial results provided by the hydroacoustic data. In the present study, a subset of cores and sub-bottom hydroacoustic data was selected, focusing on the Middle and Late Pleistocene to Holocene succession.

### *Sub-bottom profiles*

The parametric echo sounder used for this study operates with non-linear acoustics for investigating at high resolution (nominal vertical resolution <6 cm with a primary frequency around 100 kHz) the near-bottom stratigraphy (down to 50 m below the sea surface; Wunderlich & Müller, 2003). A SES 2000 Standard Plus parametric

https://doi.org/10.1017/njg.2021.3 Published online by Cambridge University Press

sub-bottom profiler (InnomarTechnologie GmbH) (average cruising speed 4.5 kn, differential GPS-based positioning) was deployed in the study area. The acoustic system allows several secondary frequencies (between 4 and 15 kHz) to be selected. Preliminary investigations close to Norderney Island indicated that maximum signal penetration occurred between 4 and 9 m, depending on the local stratigraphy. After a day-long test in the Riffgat channel, the 8 kHz secondary frequency signal was selected as being the one which would provide the best combination of penetration and resolution. Three profiles (transects 1, 2 and 3 in Fig. 1; total length 2.2 km) were processed and analysed. The ISE software (InnomarTechnologie GmbH) was used for tide correction (tidal gauge data were provided by the WSV – Wasserstraßen- und Schifffahrtsamt), speed correction (1600 m $s^{-1}$), filtering (water column removal, noise filter, stacking, and for the tracking of the hydroacoustic reflectors in specific layers. Sediment information derived from core data was imported and plotted in the ISE software. All of the depths are referred to as NHN. In some of the older studies (e.g. Keilhack & Wildvang, 1925; Dechend, 1958; Sindowski, 1973; Streif, 1990) the depth referred to NN (standard elevation zero until 2016): these depths were converted to NHN using an average of ±28 mm (LGLN, 2019).

The sub-bottom data were classified into acoustic facies based on specific properties, such as amplitude (i.e. low, moderate or high; based on the impedance contrast between beds), lateral continuity, lateral variability, depth, thickness, presence of internal structures, and the geometry of the contacts. The resulting acoustic facies were subsequently combined with the sedimentary facies information derived from the core data.

### Sediment cores and facies characterisation

In total, 16 cores were collected from the study area. The coring locations were chosen based on the crossing points of the acoustic grid and on the preliminary results of the sub-bottom data. A modified VKG 6 vibrocorer (med consultant GmbH) was deployed from aboard RV *Burchana*. The vibrocorer was used in full-load mode (1.1 t) and was equipped with PVC-liners of 5000 mm length and 100 mm diameter. The cores were cut into 1.1 m long sections, sealed, labelled and moved to the laboratory for further processing. A SeaPath System (Kongsberg Maritime) with RTK corrections (SAPOS-Service) was used for positioning.

The core sections were opened in the laboratory and high-resolution digital images were taken under constant light conditions. The cores were described following a protocol designed for the specific purposes of the WASA project (see Capperucci et al., 2021). The macroscopic description included sediment characterisation (e.g. sediment grain size, colour, sorting), sedimentary structures (e.g. lamination, lenses, evidence of reworking, bioturbation), macrofauna characterisation, presence and nature of organic matter (e.g. roots, peat layers, peat peebles), and presence of erosional contacts. The sediments were tested with dilute hydrochloric acid (10%) for carbonates.

Each core was subdivided into intervals (depositional units), based on the compositional (e.g. sediment composition, presence of fossils, carbonate content), stratigraphic (with reference to the same unit described in other cores) and geometric (e.g. sediment structures, erosional contacts) differences with the units above and below. The interpretation of the Pleistocene–Holocene deposits in the area of Norderney was based on the 140 cores collected from both offshore and from the back-barrier side of the island during the WASA project. A proper catalogue of the depositional environments and related facies was designed for this purpose, based on the detailed evidence provided by the high-resolution examination of the cores (sedimentological, stratigraphic, etc.) as well as the previously described onshore stratigraphic succession of the island. A literature review of the local deposits, extending in age from the Middle Pleistocene through to present, allowed the various depositional units to be assigned to specific depositional environments and time stages. Additionally, a fine-gravel analysis of the coarse fraction from the Pleistocene-age moraine succession was carried out in order to determine its relative age (see below).

The LBEG (Geological Survey of Lower Saxony) core database was used to extend the spatial interpretation of the Pleistocene/Holocene succession. 14 LBEG cores (available at the NIBIS® WEBSERVER website) were selected and integrated into the present study. As part of this, the sediment descriptions of the LBEG cores were reviewed and, where necessary, reinterpreted according to the WASA catalogue of the depositional environments and related facies.

### Grain-size analysis

Grain-size analysis was performed on sediment samples collected from specific core intervals, in order to aid the recognition of the various depositional environments, as well as helping to distinguish the different sedimentary facies. Since much of the sedimentary succession comprises sand and mud, the gravel fraction was not used for the grain-size determination, except for the glacial deposits, where the gravel component was treated separately and analysed in order to determine the stratigraphic age of the specific intervals (see below). The cores were sampled every 20 cm (in general), and a volume of approx. 3 $cm^3$ was used for grain-size analysis. Additional samples were collected from intervals of particular interest (e.g. corresponding to transition intervals between sub-bottom units). Samples were treated with $H_2O_2$ (15%) in order to remove the organic matter and then decalcified with HCl (10%). The samples were subsequently dispersed with sodium pyrophosphate ($Na_4P_2O_7 \times 10\ H_2O$; 1%) and placed for 24 hours on a rotation wheel. A Beckman Coulter Laserparticlesizer LS 13 320 was used for the grain-size analysis.

The results from the particle analyser were transferred into GRADISTAT (Blott & Pye, 2001) to determine the grain-size distribution and the statistical values. Mean grain size was calculated using the method of Folk & Ward (1957). Sediments were then divided into grain-size classes (from clay to coarse sand) (Table 1).

### Fine gravel analysis

In order to assess the stratigraphic age of the moraine, a fine gravel analysis according to TGL 25 232 (1971, 1980) was carried out. This analytic method is mainly used in Eastern Germany and Poland (cf. Bussemer, 2002; Börner et al., 2015; Obst et al., 2017). According to Erd (1994) and Nowel (2003), however, this method can be used more generally. For example, Ehlers (1978) successfully used a similar analysis (cf. Zandstra, 1976, 1978) on successions from Germany, the Netherlands and Denmark, suggesting that it could be used to determine the stratigraphic age of tills.

The fine-gravel analysis consists in sampling particular grain-size fractions, which are believed to represent specific bed load fractions. For this purpose, approx. 5 kg of material (corresponding to a core length of approx. 70 cm) was taken from selected cores. The samples were first dried at room temperature and weighed. Subsequently, the material was put into 30°C warm water to loosen and disaggregate the sediment. The fractions corresponding to 4–10 mm and >10 mm were then selected by wet-sieving for further investigations. The 4–10 mm fraction was used to carry out a

https://doi.org/10.1017/njg.2021.3 Published online by Cambridge University Press

**Table 1.** Mean grain-size distribution of facies F1–12 (S = sand, U = silt, C = clay; v = very, c = coarse, m = medium, f = fine)

| | F1 | | | | | | | | | | | | |
|---|---|---|---|---|---|---|---|---|---|---|---|---|---|
| | Lower part | Upper part | F2 | F3 | F4 | F5 | F6 | F7 | F8 | F9 | F10 | F11 | F12 |
| Sand | 92.6% | 61.1% | 90.1% | 72.2% | 86.2% | 94.8% | 83.1% | 95.1% | 44.6% | 46.7% | 94.4% | 89.1% | 84.9% |
| Mud | 7.4% | 38.9% | 9.9% | 27.8% | 13.8% | 5.2% | 16.9% | 4.9% | 55.4% | 53.3% | 5.6% | 10.9% | 15.1% |
| vcS | 0.0% | 0.0% | 0.0% | 0.3% | 0.0% | 0.0% | 0.0% | 0.0% | 0.0% | 0.0% | 0.0% | 0.7% | 0.0% |
| cS | 0.7% | 0.0% | 3.5% | 6.7% | 0.0% | 0.2% | 0.2% | 0.9% | 0.1% | 0.3% | 0.0% | 12.8% | 1.9% |
| mS | 18.2% | 0.0% | 12.6% | 21.6% | 0.2% | 5.5% | 1.2% | 6.5% | 2.3% | 2.6% | 1.3% | 29.0% | 22.8% |
| fS | 48.5% | 13.6% | 43.6% | 31.6% | 38.7% | 56.1% | 30.9% | 54.8% | 21.2% | 21.7% | 63.8% | 40.0% | 47.7% |
| vfS | 25.2% | 47.5% | 30.3% | 12% | 47.2% | 33.0% | 50.7% | 32.9% | 21.0% | 22.1% | 29.3% | 6.7% | 12.3% |
| vcU | 3.9% | 21.5% | 4.4% | 4.3% | 7.2% | 2.3% | 10.2% | 1.9% | 11.2% | 11.9% | 1.8% | 1.8% | 2.8% |
| cU | 0.9% | 5.2% | 1.0% | 3.7% | 1.4% | 0.4% | 1.8% | 0.5% | 12.0% | 10.8% | 0.6% | 1.6% | 2.5% |
| mU | 0.4% | 2.7% | 0.7% | 4.4% | 0.9% | 0.2% | 0.9% | 0.3% | 10.4% | 9.5% | 0.5% | 1.8% | 2.5% |
| fU | 0.4% | 2.2% | 0.7% | 4.3% | 0.9% | 0.3% | 0.8% | 0.3% | 7.4% | 7.2% | 0.5% | 1.6% | 2.3% |
| vfU | 0.4% | 1.7% | 0.6% | 3.4% | 0.8% | 0.4% | 0.7% | 0.4% | 4.7% | 4.6% | 0.5% | 1.3% | 1.5% |
| C | 1.4% | 5.5% | 2.4% | 7.8% | 2.6% | 1.5% | 2.5% | 1.5% | 9.7% | 9.3% | 1.6% | 2.8% | 3.6% |

stratigraphic analysis by separating at least 200 granules per sample into specific groups (NK = Nordic crystalline rocks; PK = Palaeozoic limestone; PS = Palaeozoic shale; D = dolomite; F = flint; MK = Mesozoic limestone; S = sandstone; Q = quartz; SO = other), where the ratio of PK, PS*10 and Ffr*10 (= unweathered flint) is used to determine the stratigraphical age (Fig. 2). The clasts larger than 10 mm ('indicator stones' in Smed & Ehlers, 2002) were used to determine the origin, and therefore to confirm the stratigraphic age, of the till. In order to be able to achieve a statistically reliable conclusion, three WASA cores in addition to core N70 were also sampled and analysed (i.e. cores N20, N22, and Nney_02).

### *GIS and graphic software*

QGis v.2.14.1 was used to plot, visualise/analyse the data (e.g. existing data sets, sub-bottom transects, core locations), and to produce the maps. The EasyCore software (The EasyCopy Company) was used to sketch the cores, and the graphic correlation of the cores was done by means of the EasyCopy software (The EasyCopy Company). The GIMP v2.8.22 and CorelDRAW Graphic Suite 2020 software were used to draw the figures.

## Results

### *Transects*

Based on the compiled lithological and hydroacoustic data (Table 2), the three high-resolution transects allowed the determined stratigraphic scheme for the Pleistocene/Holocene succession (cf. Sindowski, 1973; Streif, 1990) to be extended along the western part of the East Frisian barrier island system.

### *Hydroacoustic and lithological facies*

The detailed analysis of the hydroacoustic transects and the close examination of the sediment cores allowed 12 different facies types (F1–12) to be identified (Table 2). The facies types include deposits related to glacial and periglacial processes (i.e. moraine and outwash deposits), continental environments (i.e. lacustrine and fluvial settings), as well as marine and transitional environments (i.e. from brackish-lagoonal to intertidal and subtidal deposits). None of the Pleistocene sediments reacted with the hydrochloric acid (carbonate content = 0).

#### *F1*

Concave and oblique (divergent to planar) reflectors characterise some of the stratigraphically oldest facies (transects 2 and 3) in the acoustic data. The high-amplitude acoustic reflector at a depth of between −18 and −19 m NHN has a lateral extension of nearly 500 m on transect 3. Two cores (N24b, transect 2; N72, transect 3) correspond to this acoustic reflector. The pale brown fine sandy sediments (C: 5.5%; U: 30.8%; vfS: 47.5%; fS: 13.6% in bulk sample) contain highly organic-rich fine-grained layers (vfS with mud), the occurrence of which decreases towards the top of the depositional unit, and suggests that deposition occurred in a low-energy environment. The base of this facies is characterised by coarser sandy sediments (C: 1.4%; U: 5.9%; vfS: 25.2%; fS: 48.5%; mS: 18.2%; cS: 0.7% in bulk sample).

#### *F2*

Oblique planar reflectors characterise this facies, which suggest the possible presence of cross-stratification with transport towards the SE. A high-amplitude reflector at a depth between −17 and −18 m NHN can be laterally traced along transects 2 and 3 for approx. 350 m and 500 m, respectively. F2 was found in three cores (N74, transect 1; N24b, transect 2; N72, transect 3) and comprises pale to medium brown sands, without any internal structures (although some grading was noted). The larger amount of relatively medium to coarse-grained material within the samples (C: 2.5%; U: 7.5%; vfS: 30.3%; fS: 43.6%; mS: 12.6%; cS: 3.5% in bulk sample) and the fining-upward nature would suggest that sedimentation occurred in a moderate- to high-energy depositional system, with a decrease in energy levels towards the top of the unit. Single clasts (flint stone and quartz, average size 2.5–3.5 cm) were also found in the facies.

#### *F3*

This particular facies is delimited by two of the most prominent reflectors observed in the acoustic data set and was mapped on

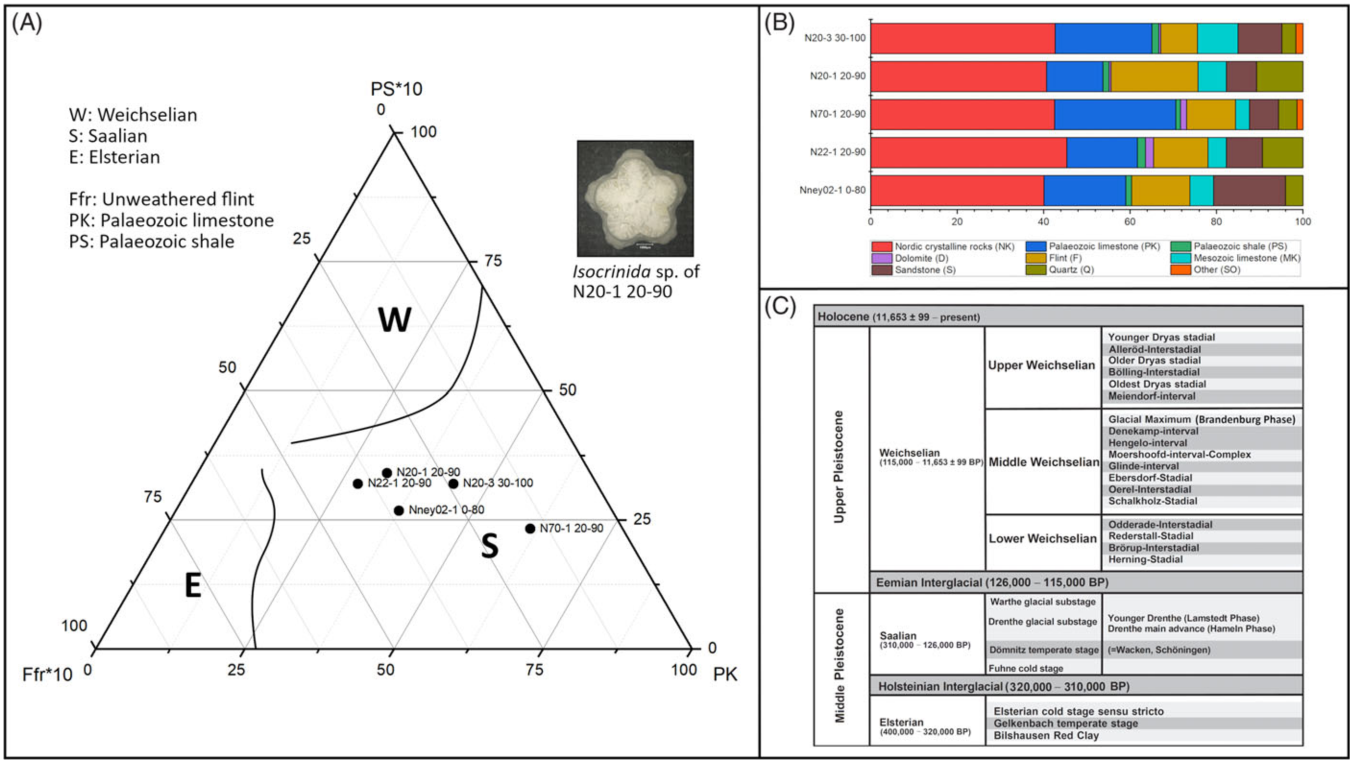


**Fig. 2.** (A) Results of the fine-gravel analysis after TGL 25 232 (1971, 1980), presented as a ternary diagram, and the crinoid *Isocrinida.* sp. (B) Percentages of gravel classes, after TGL 25 232 (1971, 1980). (C) Stratigraphy of Lower Saxony, modified from Streif (2004).

all three transects, with a lateral extent of more than 750 m (transect 1), 350 m (transect 2) and 850 m (transect 3). F3 was found in five different cores (N74, transect 1; N24b, transect 2; N70, N72 and T20, transect 3). The sediment composition includes a variety of sediments (from light grey to light green in colour), ranging from clays to cobble-grade gravels, without any evident sedimentary structure. Thus, the sediment is depicted as a diamicton. The matrix is made by sands and muds (C: 7.8%; U: 20%; vfS: 12%; fS: 31.6%; mS: 21.6%; cS: 7% in bulk sample). The fine-gravel analysis of core N70 was based on 282 granules (NK: 42.6%; PK: 28%; PS: 1.1%; D: 1.4%; F: 11.4%; MK: 3.2%; S: 6.7%; Q: 4.3%; SO: 1.4%) (Fig. 2). A rare Mesozoic-age crinoid *Isocrinida* sp. (Fig. 2) was found in the F3 facies of N20.

*F4*

Oblique planar acoustic reflectors characterise this facies. A high-amplitude reflector is recognised at a depth between −11 and −13 m NHN, and this can be laterally traced along transects 1, 2 and 3 for approx. 350 m, 150 m and 60 m, respectively. Two cores, both located within the Riffgat channel (N26, N74, transect 1), extended as far as this reflector. The sediments are characterised by planar-bedded, mica-bearing very fine-grained sands (C: 2.6%; U: 11.3%; vfS: 47.2%; fS: 38.7%; mS: 0.2% in bulk sample). Mud couplets are also present, suggesting a low-energy depositional environment. The sediments are enriched in organic content. Marine diatoms were found in core N26. The NE end of transect 1 lacks any recognisable acoustic reflectors. However, core N26 documents the presence of this facies (Fig. 3).

*F5*

This acoustic signal is quite similar to F4 and F10 and shows oblique planar geometries. On transects 1, 2 and 3 a high-amplitude reflector at a depth of between −10 and −13 m NHN can be traced laterally for approx. 1000 m, 120 m and 60 m, respectively. Four cores, located within the Riffgat channel (N26 and N74, transect 1; N18 and N71, transect 3) extend as far as the high-amplitude reflector. The sediments are characterised by planar- to cross-bedded mica-bearing fine-grained sands (average composition: C: 1.5%; U: 3.6%; vfS: 33%; fS: 56.1%; mS: 5.5%; cS: 0.2% in bulk sample), which suggests a low- to medium-energy depositional environment. The bedding, which mainly occurs in the lower part of the sequence, shows an alternation of sand layers (e.g. sample N18-1_89–90 cm, C: 1.9%; U: 6.4%; vfS: 54.3%; fS: 37.4%; mS: 0%; cS: 0% in bulk sample) with intercalated mud to sandy mud layers (sample N18-1_90–91 cm, C: 11.6%; U: 46.2%; vfS: 33%; fS: 29.9%; mS: 11%; cS: 0.5% in bulk sample). F5 can be distinguished from F4 due to its bedding type, its slightly higher content of fine- and medium-grained sands, and the negligible organic content.

*F6*

The main characteristic of this facies is the planar to concave, broadly continuous reflectors. The acoustic record shows a high-amplitude reflector at a depth of between −8.5 and −12 m NHN, which can be laterally traced along transects 1, 2 and 3 for approx. 125 m, 120 m and 50 m, respectively. Concave reflectors possibly represent channel structures. The facies is present in two cores (N18; N71, transect 3). Planar interbedded deposits of fine-grained sandy sediment (C: 2.5%; U: 14.5%; vfS: 50.7%; fS: 30.9%; mS: 1.2%; cS: 0.2% on bulk sample) suggest a moderate- to high-energy depositional environment. The sediments are cryoturbated and include evidence of root structures.

*F7*

This facies has been mainly correlated between the three transects on the basis of its stratigraphic position. On both transects 1 and 2,

**Table 2.** Facies description and stratigraphic interpretation of hydroacoustic and core data, mean grain size (S = Sand, U = silt, C = clay; v = very, c = coarse, m = medium, f = fine) after Folk & Ward (1957). Ages from radiocarbon dating. Ages of peat were provided by Schlütz et al. (2021)

| Facies | Hydroacoustic investigation | | | Lithological investigation | | | | | | | | |
|---|---|---|---|---|---|---|---|---|---|---|---|---|
| | Transect | Amplitude | Reflective pattern | Core | Thickness (cm) | Mean grain size | Sedimentary structures | Carbonate content | Colour | Content/components | Stratigraphic interpretation | Dating |
| F12 | 1, 3 | High | Individual moderate- to high-amplitude reflectors, broadly continuous, both planar and concave, parallel behaviour | N26, N70, T20 | 1–140 | fS | Massive to cross- to planar-bedded | High | Grey | Shells, small cobbles | Holocene channel fill | — |
| F11 | 1, 3 | High | Very high amplitude, reflective surface, laterally traceable, planar structure | N26, N70, N72, T20 | 1–10 | fS | Chaotic | High | Grey | Well-rounded cobbles, highly fragmented shells | Holocene channel lag | — |
| F10 | 3 | Moderate | Individual moderate-amplitude reflectors, oblique planar | N26 | 107 | vfS | Cross-bedded, planar bedded towards the top | Low | Grey | Mud couplets, crumbled peat | Holocene sand flat | *Cerastoderma edule:* 2260 ± 30 yrs BP |
| F9 | 1, 2, 3 | Moderate | Individual moderate- to high-amplitude reflectors, moderate continuous, tend to be parallel-planar | N18, N71 | 17.5–75 | vcU | Laminated | — | Grey-brown | Roots | Holocene lagoonal deposits | — |
| F8 | 1, 2, 3 | High | Very high amplitude, reflective surface, laterally traceable, planar structure | N18, N71 | 5–20 | — | Massive to bedded | Very low | Dark brown | Sandy beds, plants, roots | Holocene peat | Peat: 7630 yrs BP (N18), 7780 yrs BP (N71) |
| F7 | 1, 2, 3 | Low | Low-amplitude reflectors, broadly concave, chaotic pattern | N18, N71 | 40–84.5 | fS | Massive, fining upwards | – | Dark brown | Highly humic, organics, plants, reed rhizomes, mica | Weichselian crevasse splay deposits (with palaeosol) | — |
| F6 | 1, 2, 3 | Moderate | Individual moderate- to high-amplitude reflectors, broadly continuous, tend to be planar to concave | N18, N71 | 222–240 | vfS | Planar bedded, cryoturbated, normal grading | – | Light grey | Mica, roots | Weichselian fluvial deposits | — |
| F5 | 1, 2, 3 | Moderate | Individual moderate-amplitude reflectors, oblique planar | N18, N26, N71, N74 | 80–160 | fS | Planar bedded, cross-bedded towards the top | — | Greenish-grey | Mica, diatoms | Eemian sand flat | — |
| F4 | 1, 2, 3 | Low–moderate | Individual moderate-amplitude reflectors, oblique planar | N26, N74 | 65–149 | vfS | Planar bedded | — | Greenish-grey | Mud couplets, mica, diatoms | Eemian mixed flat | — |

**Table 2.** (*Continued*)

| | | | | | | | | | | | | |
|---|---|---|---|---|---|---|---|---|---|---|---|---|
| F3 | 1, 2, 3 | Moderate | Chaotic, reflective pattern, individual moderate-amplitude reflectors, discontinuous and show no signs of any parallel behaviour | N24b, N70, N72, N74, T20 | 136–316 | vfS | Massive | Low | Olive-grey-brown | Well-rounded flints, chalks and igneous rocks | Saalian moraine (Drenthe Main Till) | Saalian (fine-gravel analysis) |
| F2 | 1, 2, 3 | Low–moderate | Individual low-amplitude reflectors, broadly continuous, oblique planar | N24b, N72, N74 | 30–150 | fS | Massive to weakly bedded, fining upwards | Very low | Grey-brown | Flints, siliceous gravels | Saalian outwash deposits (sandur plain) | — |
| F1 | 1, 2, 3 | Low | Individual reflectors, both oblique divergent to planar, moderately continuous, broadly concave | N24b, N72 | 124–135 | vfS | Weakly bedded | Very low | Greyish to greyish-brown to brown | Detrital plant fragments | Middle Pleistocene lacustrine-deltaic deposits | — |

the facies lacks any clear reflectors, while on transect 3 concave reflectors are recognised. F7 is present in cores N18 and N71 of transect 3. The highly organic-enriched fine-grained sands (C: 1.5%; U: 3.5%; vfS: 32.9%; fS: 54.8%; mS: 6.5%; cS: 0.9% in bulk sample) decrease in grain size toward the top of the unit (fining upward) and are mostly structureless, indicating a depositional system with varying or decreasing energy levels. The facies includes highly decomposed plant fragments and also shows evidence of root penetration. The amount of organic content increases towards the top, as shown by the change in colour, which ranges from golden brown (basal part of F7) grading to dark brown (humic fine sand, top of the unit). The top of the unit is usually in direct contact with F8.

*F8*

The facies is marked by a highly recognisable high-amplitude reflector in all three transects at a depth of −6 m and −7 m NHN in transects 1 and 2, respectively, and at a depth of −9 and −10 m in transect 3. It can be traced laterally along transects 1, 2 and 3 for approx. 125 m, 120 m and 20 m, respectively, and is often associated with the intercalated deposits of F9. Two cores (N18 and N71) showed the presence of this facies in transect 3. The deposits comprise mainly peat, with a varying amount of sand (S: 5.6–83.7% in bulk sample) and the presence of reed rhizomes.

*F9*

Continuously parallel-planar reflectors characterise this facies along all three transects. The facies is intercalated with the peats of F8 and can therefore easily be identified at depths of −6 m and −7 m NHN in transects 1 and 2, and at a depth of −9 and −10 m in transect 3. It can be laterally traced along transects 1, 2 and 3 for approx. 125 m, 120 m and 20 m, respectively. Cores N18 and N71 (transect 3) contain this facies, which is characterised by organic-enriched laminated muddy sediments (C: 9.3%; U: 44%; vfS: 22.1%; fS: 21.7%; mS: 2.3%; cS: 0.3% in bulk sample), suggesting a low-energy depositional environment.

*F10*

This facies is similar to F4 and F5 and is characterised by oblique planar reflectors. These are noted at the NE end of transect 1. The facies is associated with the deposits of F11 and F12 and can therefore easily be localised at depths of between −11 and −13 m NHN with a lateral extension of almost 350 m. F10 is only present in core N26. The sediments are characterised by cross- to planar-bedded, fine-grained sands (C: 1.6%; U: 4%; vfS: 29.3%; fS: 63.8%; mS: 1.3%; cS: 0% in bulk sample), which indicate a low- to medium-energy depositional environment. The facies is distinguished from F4 and F5 by the presence of crumbled peats and the lack of mica. A specimen of the cockle *Cerastoderma edule* was found in life position and was dated at 2260 ± 30 yrs BP, using the radiocarbon method.

*F11*

The facies comprises a high-amplitude reflector in transect 1 at a depth of −12 to −13 m NHN, which can be laterally traced along the transect for approx. 150 m. The facies is present in four cores (N26, transect 1; N70, N72, T20, transect 3). The transition to F11 is usually marked by the presence of a chaotic coarse-grained layer, with reworked shells and shell fragments in a matrix of sand to gravel (fine fraction: C: 2.8%; U: 8.1%; vfS: 6.7%; fS: 40%; mS: 29%; cS: 13.5% in bulk sample).

https://doi.org/10.1017/njg.2021.3 Published online by Cambridge University Press

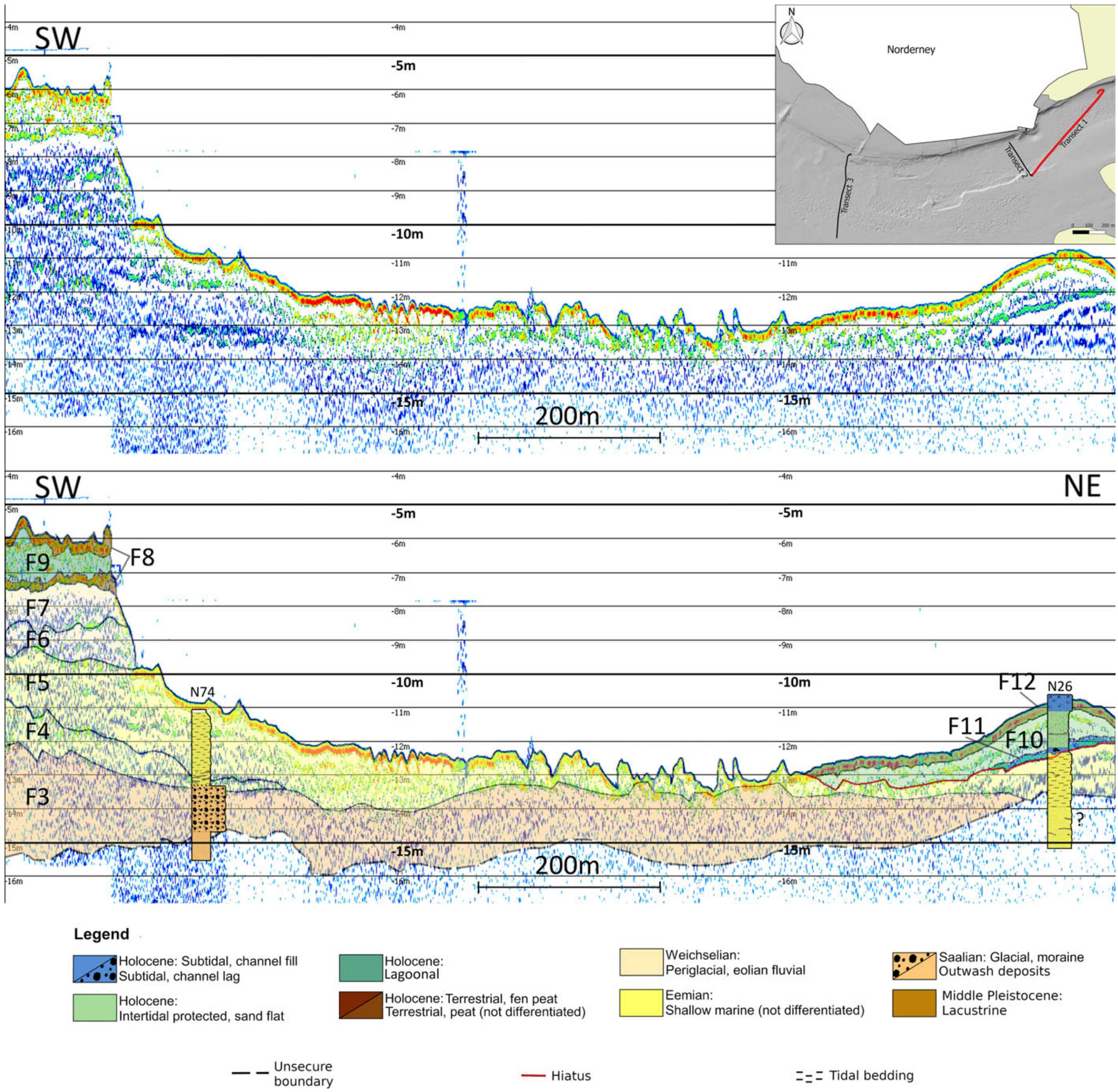


**Fig. 3.** Transect 1 sub-bottom profile (top) crossing the Riffgat channel and its interpretation (bottom). The Pleistocene sequence starts with the Saalian moraine (F3). Eemian tidal flat deposits (F4 and F5) are well shown in this transect. Core N26 confirms the presence of a thick Eemian succession for the NE end of transect 1, though no reflector was detected. Depth refers to NHN. For the description of the facies, see Table 2.

*F12*

Broadly continuous reflectors, which are both planar and concave, are characteristic of this facies (e.g. transects 1 and 3). The depth of the high-amplitude reflector varies from −7 to −15 m NHN, and it can be laterally traced along transects 1 and 3 for approx. 350 m and 600 m, respectively. The base of the facies comprises high-amplitude reflectors, which may represent a lag deposit (i.e. AF11). Three cores (N26, transect 1; N70; T20, transect 3) were collected, which contain this facies. The sediments are characterised by massive to cross- to planar-bedded, fine-grained sands (C: 3.6%; U: 11.5%; vfS: 12.3%; fS: 47.7%; mS: 22.8%; cS: 1.9% in bulk sample) as well as shells and some small cobbles, indicating deposition in a moderate- to high-energy depositional environment.

## Discussion

The compilation of new data of high-resolution sub-bottom hydroacoustics and vibrocores (up to 5 m length) collected as part of this study has allowed a better understanding of the stratigraphy of such key area for the reconstruction of the Middle Pleistocene to early Holocene history of the region. This builds on work carried out by a number of studies which commenced in the 1950s (e.g.

Dechend, 1950, 1952, 1954, 1958) and is still ongoing (e.g. Streif, 1990, 1998, 2004; Hoselmann & Streif, 2004). The new and extremely detailed data set also demonstrates the complexity of the Pleistocene palaeorelief and the lateral heterogeneity of the Holocene deposits for the western part of the East Frisian Wadden Sea.

### Facies interpretation

A total of 12 different facies have been identified from the three sub-bottom transects and a range of core data (see above for details). In contrast to the historical published data (e.g. Sindowski, 1973; Streif, 1990), the use of hydroacoustic data allows to extend the knowledge about the presence of the Middle Pleistocene- and Eemian units across a much broader area. In this subsection the facies types are discussed in detail.

#### F1 – lacustrine-deltaic deposits

This facies represents the oldest deposits found in the cores. The stratigraphic position of these sediments (underneath the Saalian moraine, see F3), together with their sedimentological characteristics, differs from those of similar deposits described in the literature for the same area (e.g. Sindowski, 1973) and would suggest that they represent Middle Pleistocene (most likely Holsteinian or Dömnitz temperate stage) lacustrine-deltaic deposits. In F1, the presence of both coarse- and fine-grained sediments suggests a variety of depositional settings, coexisting on a small scale during the transition between the temperate stage (either Holstein or Dömnitz temperate stage) and the subsequent Saalian glacial phase. The coarser-grained sediments may therefore represent either a distributary channel infill or a sandy mouthbar deposit, while the fine-grained deposits may represent deposition within an interdistributary bay, which developed as a swampy delta plain under subaerial conditions (cf. Lang et al., 2012, 2015; Hepp et al. 2019). Lacustrine deltas within Elsterian tunnel valleys have been recorded by a number of authors from Northern Germany (Ehlers & Linke, 1989; Streif, 1990; Lutz et al., 2009; Stackebrandt, 2009).

#### F2 – outwash deposits (sandur plain)

The facies is considered to represent Saalian-age proglacial outwash deposits (cf. Ehlers, 1990; Eissmann, 2002; Hambrey, 2007). The sediments are broadly fining upwards and show cross-stratification with transport towards the SE. Thus, the sediments are interpreted as channel deposits. Furthermore, the observed clasts (e.g. flints) within the sediments are very similar to the fine-grained gravels of the overlying till deposits of F3, indicating a coherent evolution (i.e. a sandur plain located at the ice margin). In the Saalian period, three glaciations occurred, although only the older Main Drenthe advance (Older Saalian Glaciation) affected the area of Norderney (Ehlers, 1990). During this phase, a glacio-fluvial system developed (Streif 1990) and the outwash sands have been described as containing flints and siliceous gravels (Eissmann, 2002). It is therefore highly probable that the deposits of this unit were formed on the sandur plain of the Main Drenthe advance, particularly since the overlying moraine is also identified as the Drenthe Main Till.

#### F3 – moraine

The facies was interpreted as the Older Saalian Till (i.e. Drenthe Main Till), the deposits of which can be found extensively in Northern Germany (cf. Rappol et al., 1989; Eissmann, 2002; Meyer, 2005; Lambeck et al., 2006). The F3 facies closely resembles the boulder clay described by Streif (1990) as greyish-green to brownish-grey sediments with an average thickness of 1–5 m (maximum thickness 10 m). The moraine in the core data shows a thickness between 1.4 and 3.2 m. The fine-gravel analysis conducted on the coarser fraction of the moraine confirmed the age as Saalian (Fig. 2). Based on the proven efficacy of the similar methodology of Zandstra (1978) for Northern Europe (see Ehlers, 1978, 1980 for Germany; Zandstra, 1976 for Northern Netherlands; and Ehlers, 1979 for Denmark), we would suggest that the TGL 25 232 (1971, 1980) is a suitable method to determine the stratigraphic age of tills in Lower Saxony. The >10 mm fraction consists of crystalline detritic material with an origin in central to eastern Sweden (cf. Smed & Ehlers, 2002).

#### F4 – tidal flat deposits I

This facies was interpreted as representing Eemian-age mixed tidal-flat deposits, based on the presence of interbedded tidal bundles. This interpretation differs from the more generalised description of a sandy tidal flat of previous authors (e.g. Dechend, 1954; Sindowski, 1973; Streif, 1990). In tidal-flat systems, energy conditions are variable, with energy levels generally increasing towards the open sea. With such an increase in energy, the levels of organic matter and mud within the sediment decrease as a result of winnowing (cf. Fan, 2012; Flemming, 2012). Based on the results of the grain-size analysis (i.e. low percentages of mS and a lack of cS) the sediments may represent a mixed-flat environment (cf. Flemming, 2012). Within this facies, the sand/mud ratio (6:1) is very high. Thus, it can be concluded that the sediments were deposited in a more exposed environment, which could have been either an external part of a mixed flat or a transition zone from a mixed flat towards a sand flat. The sediments in F4 correspond to modern tidal-flat deposits observed in the same area, suggesting the presence of similar depositional conditions (cf. Sindowski, 1973; Streif, 1990; Caspers et al., 2002; Shackleton et al., 2003; Schokker et al., 2004; Leduc et al., 2010).

#### F5 – tidal-flat deposits II

The facies was interpreted as Eemian-age sand-flat deposits. F5 is quite similar to F4, though the sediments of F5 are slightly more coarse-grained. The mud content is >5% while the amount of organic matter is negligible. The sediments of F5 are considered to have been deposited under medium energy conditions, and represent either an external part of the Eemian sand-flat environment or a transition zone from a sand flat towards a mixed-flat environment (cf. Flemming, 2012).

#### F6 – fluvial deposits

This facies is interpreted as Weichselian-age fluvial deposits. Internal concave reflectors are interpreted as channel structures. Additionally, the sediments show evidence of normal grading, which is also typical for channel deposits. This facies is associated with the deposits of F7, which are interpreted as crevasse splay deposits. These combined characteristics led to the interpretation that these deposits represent a meandering river system. The presence of cryoturbation features provides evidence that the sediments were deposited under permafrost conditions. The channel (or channels?) was oriented EW based on the orientation of the concave reflectors in all three transects. During the Weichselian, although the area of Norderney was not covered by ice, glacial climatic conditions were active (Boulton, 2001; Knies et al., 2001). Thus, periglacial processes were common (Huijzer &

Vandenberghe, 1998). Meandering river systems with crevasse splays (F7) developed in Northern Germany as noted by previous authors (van Huissteden et al., 1986; van Huissteden, 1990; Vandenberghe & Woo, 2002). The deposits of these rivers have been described by Streif (1990) as fine sands and silts, which are brownish-grey and are interbedded with medium-grained sands, gravels and plant fragments. In addition, periglacial features such as ice wedges or solifluction are quite common (Streif, 1990), both of which were also recognised as part of this study.

*F7 – crevasse splay deposits (with palaeosol)*

The facies was interpreted as Weichselian-age continental deposits (i.e. semi-terrestrial, as a result of the transition from the Eemian shallow-marine environments to the Weichselian proglacial conditions). Van Huissteden (1990) described similar Weichselian-age sediments from the Northern Netherlands, and interpreted them as crevasse splay deposits. His interpretation is consistent with the sedimentological characteristics observed in F7 (sandy sediments, fining upward) and with the interpretation given for F6 (fluvial deposits). Several authors (e.g. Dury, 1964; van Huissteden et al., 1986; van Huissteden, 1990; Vandenberghe & Woo, 2002) showed that crevasse splays develop within a fluvial system, independent of the climatic conditions. The topmost part of this facies is rich in organic matter (humus, detritus, roots). The organic enrichment was probably a result of post-diagenetic pedogenic processes, which occurred during the final stage of the Weichselian/early Holocene phase. According to Kraus & Aslan (1993) and Collinson (2009) the top of F7 can be described as simple alluvial palaeosols (weak development of horizons, A-horizon very rare, colours from grey to yellow-brown, diffuse presence of roots). It has been noted that such palaeosols may develop in crevasse splays (Collinson, 2009; Gulliford et al., 2017).

*F8 – peat*

This facies was interpreted as Holocene peats. The Holocene succession of the Wadden Sea commences with the formation of a basal peat, which developed due to the rising groundwater table, and which was associated with an increase in swampy conditions and the development of mires (cf. Streif, 1990, 2004). Based on the presence of reed rhizomes within F8 sediments, it was possible to identify the peat of core N71 as a fen peat. These peat deposits are partly intercalated with fine- to very fine-grained sands and muds. The clastic material may have been deposited as a result of aeolian sediment transport (loess or wind-blown sand). The basal peats in cores N18 (7630 yrs BP), N71 (7780 yrs BP) and N23 (6850 yrs BP) were dated by Schlütz et al. (2021).

*F9 – brackish-lagoonal deposits*

Brackish-lagoonal or lacustrine sediments are deposited under similar conditions and are not easily distinguishable (Nichols, 2012). However, analysis of diatoms from this facies implies a brackish environment, and thus it can be suggested that this facies represents a Holocene brackish-lagoonal depositional system. Such settings were quite common in the North Sea area during the early Holocene, when fens and bogs started to develop (Streif, 1990, 2004).

*F10 – tidal flat deposits III*

The facies was interpreted as Holocene sand-flat deposits. As noted above, the marine bivalve *Cerastoderma edule* (dated at 2260 ± 30 yrs BP), also known as the common cockle, was found in life position in core N26. This bivalve is typically found in shallow-marine environments. According to Fan (2012), the presence of mud couplets is one of the main criteria for recognising tidal-flat environments. A second criterion, according to Fan (2012), is the presence of cross-bedding structures. F10 comprises mud couplets and shows evidence of weak cross-bedding, which changes to parallel bedding towards the top of the facies. The change in bedding type can result from variations within the energy levels. In a sand-flat environment only <5% of mud is generally present (Flemming, 2012). This corresponds to the sediment characteristics of this facies.

*F11 – channel lag deposits*

This facies was interpreted as a channel lag deposit comprising coarse-grained sediments, mainly sands and gravels, as well as chaotic deposits. Such deposits are typically present at the base of subtidal channels within the tidal-flat environment (e.g. Fan, 2012; Flemming, 2012). Streif (1990) noted the presence of coarse-grained sands and gravels at this stratigraphic level. He also noted that the unit contained shell fragments. Such lags are typical of tidal-flat successions (cf. Flemming et al. 1992; Scasso et al. 2012).

*F12 – channel fill deposits*

Channel fill sediments overlie the channel lag deposits (F11) and, together, form a typical tidal channel sequence (cf. Flemming, 2012). The extensive presence of cross-bedding and planar bedding structures in the cores, together with the grain-size characteristics of these sediments (fine-grained sandy sediments with mud layers, occasionally interbedded with coarse-grained sediments and shell/gravel lags), suggests that deposition occurred in an environment characterised by alternating high- and low-energy conditions, which is consistent with a channel fill system (cf. Fan, 2012; Flemming, 2012).

### Stratigraphic succession: from Middle Pleistocene to early Holocene

Based on the analysis of the 12 sedimentary facies and on their correlation with the hydroacoustic profiles, a new and much more detailed reconstruction of the stratigraphy of the back-barrier area of Norderney from the Middle Pleistocene through to the early Holocene has been performed.

The deep erosion of the main tidal Riffgat channel into the Holocene and Pleistocene sediments has allowed the entire succession extending from pre-Saalian (possibly Holsteinian) lacustrine deposits through to Saalian periglacial and moraine sediments to be examined (Figs 3–5). Along the channel margins, the depositional transition from interglacial Eemian sediments to periglacial and fluvial Weichselian sediments was followed by the deposition of a transgressive sequence corresponding to the first stages of the early Holocene sea-level rise (Figs 3–5). The stratigraphic succession from the northern side of the Riffgat channel is complete (i.e. from F1 to F12), extending from the Middle Pleistocene up to the early Holocene (transect 3, Fig. 5). The successions from the southern side of the Riffgat channel (i.e. transects 1 and 2, Figs 3 and 4) are less complete, but very similar.

The reconstructed stratigraphic succession commences with lacustrine-deltaic sediments (F1) at a depth of −18 m NHN (transect 3 and lowest section of core N72), and −17 m NHN (transect 2 and core N24b), interpreted as Middle Pleistocene deposits. F1 is capped by a semi-horizontal erosional contact and overlain by around 2 m of Saalian outwash deposits (F2). The top and bottom

https://doi.org/10.1017/njg.2021.3 Published online by Cambridge University Press

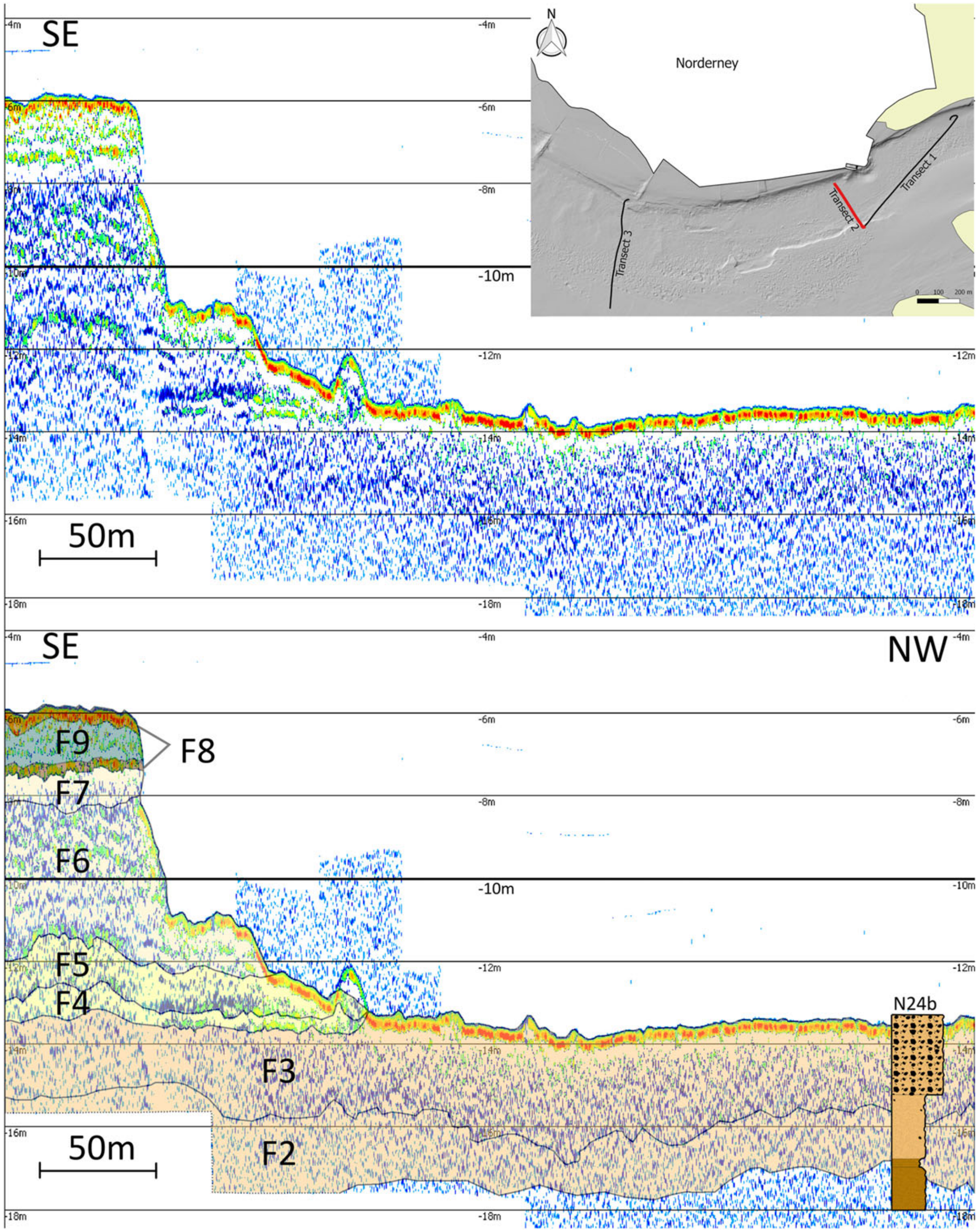


**Fig. 4.** Transect 2 sub-bottom profile (top) perpendicular to the Riffgat channel, and its interpretation (bottom). The Saalian outwash deposits (F2) are followed by the Saalian moraine (F3), which works as a limiting erosional element for the evolution of the Riffgat channel. Core N24b confirms the presence of Middle Pleistocene sediments (F1) below the Saalian deposits, though no related reflector was detected. Depth refers to NHN. For the description of the facies, see Table 2. For legend see Figure 3.

boundaries of F2 are clearly visible in the hydroacoustic data in transect 3, while on the other transects the presence of this facies is mainly deduced from the core sediment analysis (core N24b, transect 2 and core N74, transect 1). The Saalian moraine deposits (i.e. Drenthe Main Till, F3) are present in all three transects. Indeed, much of the sea floor in the main channel is covered by this coarse-grained material (i.e. medium- to coarse-grained sand and gravels). The acoustic reflector of the Saalian moraine is one of the most prominent acoustic elements, and can be identified by its clear upper and lower boundary reflectors. The Saalian moraine is overlain by 2 m of Eemian mixed-flat (F4) and sand-flat deposits (F5). The Eemian deposits are overlain by 2 m (transect 3) to 5 m (transect 2) of Weichselian fluvial (F6) and crevasse splay (F7) sediments on the margins of the Riffgat channel. A basal peat

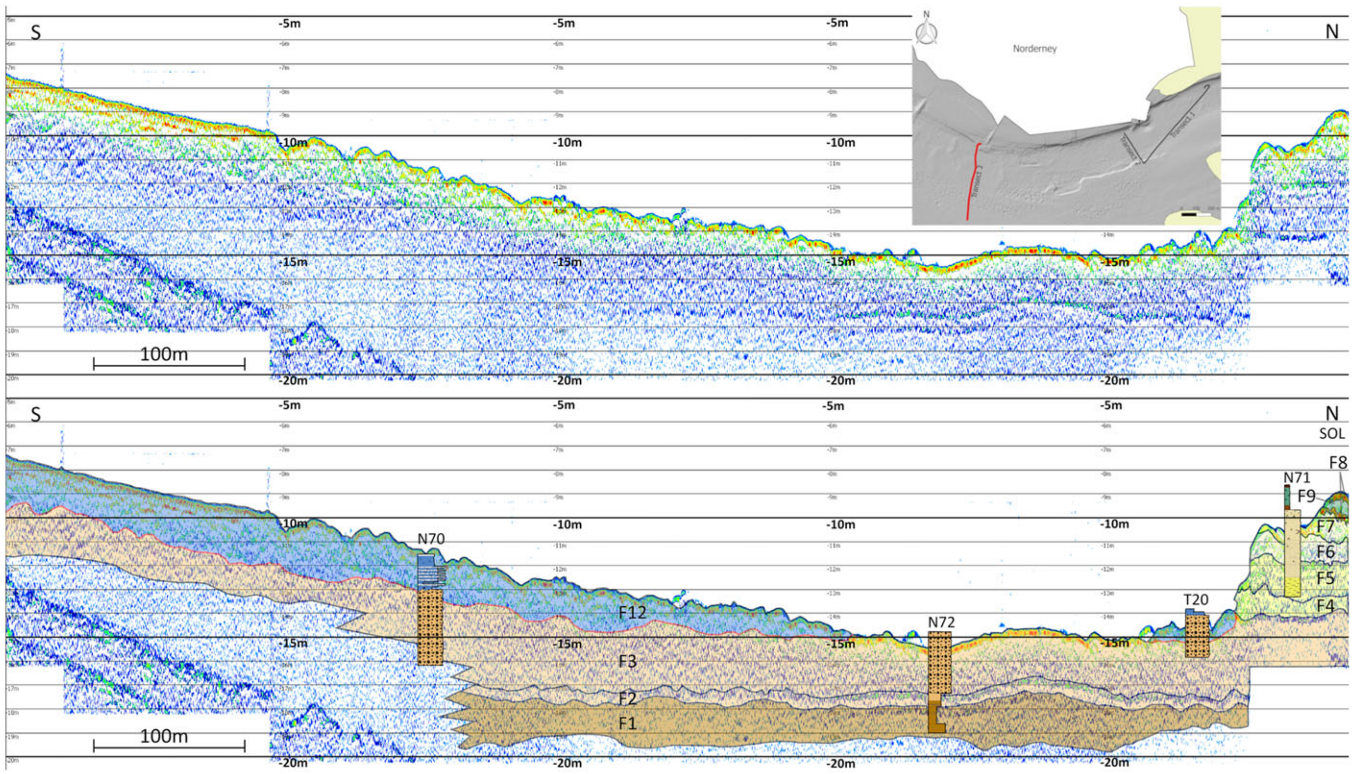


**Fig. 5.** Transect 3 sub-bottom profile (top) perpendicular to the Riffgat channel. Middle Pleistocene deposits (F1) commence the Pleistocene sequence. The Saalian moraine (F3) builds up parts the present sea floor, which works as a limiting erosional element for the evolution of the Riffgat channel. It is covered by a thick succession of Holocene subtidal channel fill deposits (F12) in the southern part of transect 3. Depth refers to NHN. For the description of the facies, see Table 2. For legend see Figure 3.

(F8) overlies the Weichselian deposits at a depth of −7.5 m (transect 1) to −10 m (transect 3) NHN, followed by brackish-lagoonal deposits (F9) and a second peat layer (F8).

In order to trace the lateral extent of our new detailed reconstruction of the stratigraphy of the western head of the island of Norderney, core data from the LBEG were included (Fig. 6). In contrast to the interpretation of Sindowski (1973), the Middle Pleistocene lacustrine facies and an Eemian shallow-marine facies are now also documented beneath the western part of Norderney. This is a significant finding, since it suggests that the profile of Sindowski (1973) is erroneous, at least in terms of describing the stratigraphy in the western part of Norderney. In addition, our high-resolution analysis of sedimentological data, such as tidal bedding and bundles, and the occurrence of marine diatoms, proves the presence of Eemian-age sediments at a depth of −10.6 m (N18) to −12,3 m NHN (N26). These new results confirm the conclusions of Dechend (1950, 1952, 1954, 1958) while disproving the interpretation of Sindowski (1973) and Streif (1990) who had suggested that Eemian deposits were completely eroded in the western area of Norderney.

### *Middle Pleistocene deposits and the presence of tunnel valleys below Norderney*

A unit of Middle Pleistocene sediments (F1) was found at a depth of −17.9 m (core N24b) and −16.8 m NHN (core N72). In addition, these deposits were present in transect 3 (Fig. 5). This facies is interpreted as lacustrine-deltaic deposits, where coarser-grained sediments represent either a distributary channel infill or a sandy mouthbar deposit, while the fine-grained deposits may result from deposition within an interdistributary bay (i.e. swampy delta-plain; subaerial conditions). Based on their potential stratigraphic position (see below), these sediments are considered to be indicators for the presence of tunnel valleys, since they have been used by various authors (e.g. Ehlers & Linke, 1989; Streif, 1990; Lutz et al., 2009; Stackebrandt, 2009; Kehew et al., 2012) to mark the uppermost unit of the infill of Elsterian tunnel valleys in Northern Germany. These tunnel valleys developed subglacially, i.e. beneath ice masses (Kehew et al., 2012).

The Elsterian tunnel valleys of Northern Germany have been mapped by Stackebrandt (2009) who noted that their NS orientation is influenced by the so-called NW German ice stream, i.e. the broad orientation of ice movement during the Pleistocene (cf. Stackebrandt et al., 2001). Stackebrandt's (2009) map indicates the presence of Elsterian tunnel valleys to the south of Norderney, the closest approx. 30 km to the south. However, the map does not indicate the presence of any tunnel valley in the Wadden Sea area. An alternative map of the Elsterian tunnel valleys in the southern North Sea has been published by Lutz et al. (2009). This map is more detailed with regard to the German North Sea sector than that of Stackebrandt (2009). It also indicates the presence of four to five tunnel valleys located approx. 5 km north of Norderney. Both of these results are in agreement with the large number of Pleistocene tunnel valleys recorded by Huuse (2000) in his comprehensive study of the tunnel valleys of Northern Europe. Thus, it can be reasonably assumed that the valleys located offshore were originally part of a broader system of subglacial valleys which extended onshore, connecting with the ones on the mainland. The broad NS orientation which has been noted from the onshore subglacial tunnel valleys would thus have continued into the offshore areas.

Subsequent to the retreat of the Elsterian ice masses, tunnel valleys functioned as locations of sediment preservation during phases of glacial and interglacial climate conditions throughout

https://doi.org/10.1017/njg.2021.3 Published online by Cambridge University Press

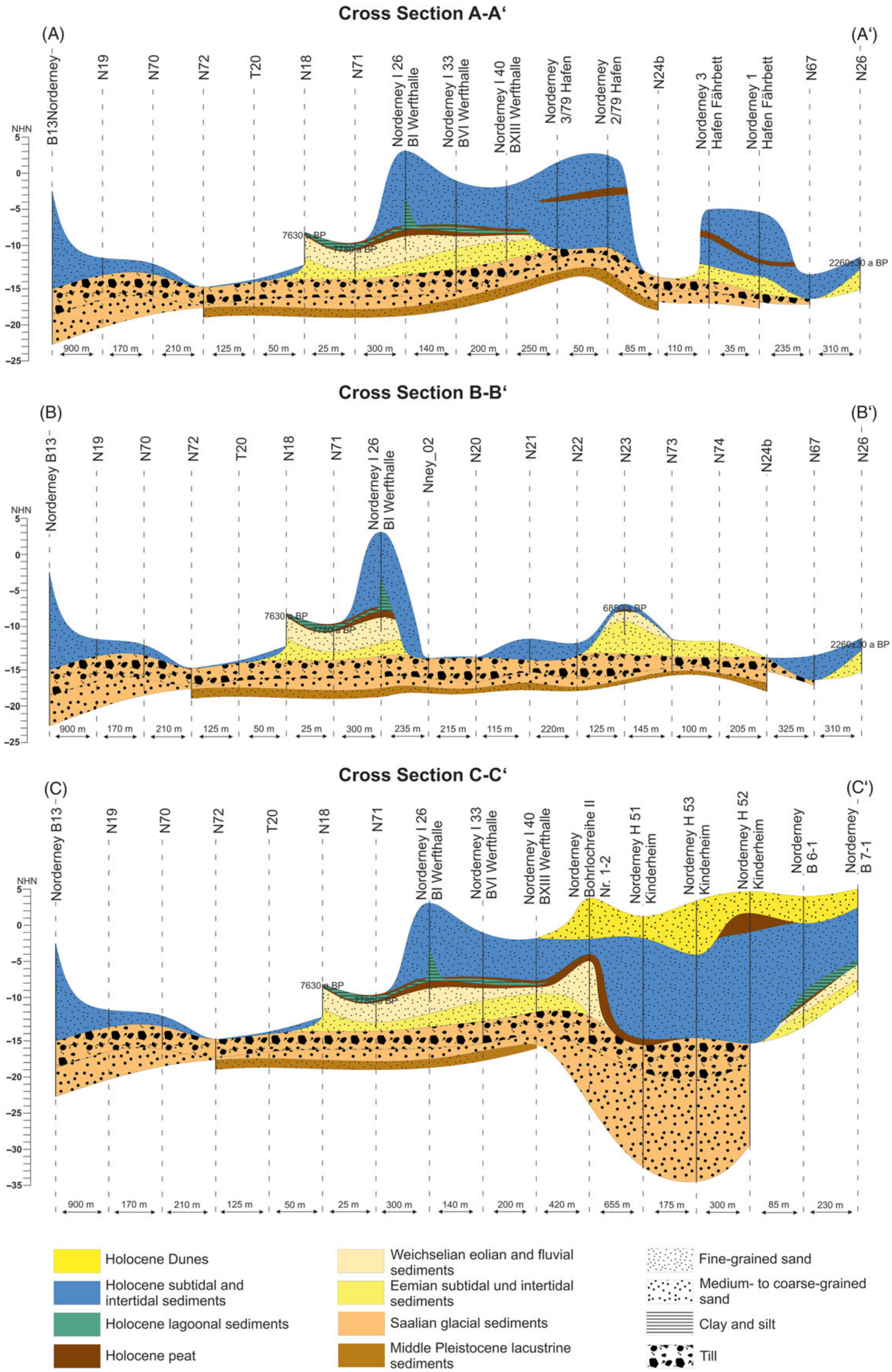


**Fig. 6.** Cross-section of the Riffgat channel (A–A′, B–B′) and the western head of Norderney (C–C′), derived from both WASA- and reinterpreted LBEG cores. For orientation of cross-sections see Figure 1.

https://doi.org/10.1017/njg.2021.3 Published online by Cambridge University Press

the Middle Pleistocene. According to Lutz et al. (2009), the sedimentary infill of the tunnel valleys is dependent on their size, with smaller valleys containing mainly homogeneous infill, while the infill within the larger valleys is mainly heterogeneous, documenting multiple depositional and erosional events. The uppermost facies present within the tunnel valley successions is interpreted as comprising stacked lacustrine delta deposits (e.g. Lang et al., 2012, 2015), which is supported by our interpretation of F1. The deposits of F1 may be stratigraphically correlated with either the Holsteinian (a) or the Dömnitz temperate stage (b), which are described in the following:

a) *Holsteinian lacustrine facies*. The Holsteinian transgression did not extend as far as the area of Norderney (Knudsen, 1988; Streif, 1990, 2004). Coeval deposits located to the south of Norderney have been described by Litt et al. (2007) as fluvial and lacustrine. The sediments are described as mainly silt and clay, and may contain diatoms (Unger et al., 1995). Both Unger et al. (1995) and Litt et al. (2007) have also suggested that the deposition of the Holsteinian lacustrine facies occurred across the broader East Frisian area and was preserved in the older Elsterian tunnel valleys. Hepp et al. (2012) recently described very similar deposits, also of Holsteinian age, preserved within an Elsterian tunnel valley in the southern North Sea.
b) *Dömnitz temperate stage* (also Wacken/Schöningen temperate stage). A succession of lacustrine deposits present across Northern Germany have been interpreted as representing the Dömnitz temperate stage (e.g. Litt et al., 2007; Urban, 2007; Urban et al., 2011; Stephan et al., 2012). Urban (2007) describes a unit of mud and peat, which developed under swampy conditions at the location of the Elsterian-age Schöningen tunnel valley (Lower Saxony, Germany). Lang et al. (2012, 2015) examined this succession and reinterpreted the sediments as shallow lacustrine delta deposits, based on extensive investigation of seismic and core data. Urban et al. (2011) and Stephan et al. (2012) described a similar sedimentary succession (which is also similar to that described in this study) from the area of Leck (North Frisian area).

Based on the overall similarity of the sediments (vfS), the facies architecture (i.e. a stacked lacustrine delta) and the depth (−17.9 to −16.8 m NHN) of the deposits, it is concluded that F1 correlates more likely to the Dömnitz temperate stage.

In conclusion, it cannot be proven with any certainty that tunnel valleys exist below the island of Norderney, based on the data set from this study. However, Middle Pleistocene deposits considered to be indicators for the presence of tunnel valleys were found below the western part of Norderney. Transect 3 shows the wide distribution of these Middle Pleistocene deposits over some hundreds of metres (Fig. 5).

### The Pleistocene–Holocene boundary

The landscape relief at the end of the last glacial period (Weichselian) was reshaped during the Holocene. New channels cut into the Pleistocene deposits and existing channel systems were reactivated, deepened and shifted during the Holocene sea-level rise. The precise morphology and depth of the Pleistocene–Holocene boundary and the composition of the overlying Holocene deposits are of particular relevance not only for scientific purposes, but also for planning and managing conservation and development in the coastal region of NW Germany (e.g. offshore wind parks cables and energy/water pipelines from the mainland to the Frisian Islands).

In order to define the morphology of the Pleistocene–Holocene boundary and to reconstruct the related palaeogeographical maps, information about the geological preconditions of the pre-existing landscape (mainly Pleistocene) can be useful. This is especially interesting with regard to resistance to erosion or reworking of previously deposited sediments. Based on both transects and cross-sections from our study, it would appear that the deposits of the Saalian moraine (i.e. Drenthe Main Till) limited the depth of the Riffgat channel. The channel does not appear to cut into the Saalian moraine, but only partially erodes the top of it. However, this situation can only be determined for the 3.5 $km^2$ of the study area. Further research is needed to analyse the limiting impact of the Saalian moraine (at varying depths) on lateral changes in the main channel (or channel system). Such information will be important for prediction of channel shift with regard to ongoing sea-level rise and predicted rises of the tidal range.

#### Reconstruction of the local palaeolandscape evolution

Based on our analysis of the geometries of the acoustic reflectors, interpreted as deltaic channels and swampy delta plain deposits (F1), a WE-oriented prograding lacustrine delta environment is suggested for the Middle Pleistocene of the Nordeney area (Fig. 7A). This interpretation is supported by detailed analysis of core N72 (i.e. western to core N24b), which contains deposits indicative of a swampy delta plain. In addition, sediments within core N24b have been interpreted as representing a deltaic channel.

Within the channels of the Saalian sandur plain (F2), downstream-migrating structures, e.g. cross-stratification, are present as oblique planar reflectors in transect 2, indicating that the sediment transport direction (cf. Scherer et al., 2015) was from NW to SE. This would confirm the results of several authors such as Ehlers et al. (2011) (Fig. 7B).

The base of the Eemian deposits in the study area documents a transgression, with the presence of a mixed tidal-flat system (F4), overlain by a sand tidal-flat system (F5) (Fig. 7C). This configuration is interpreted as representing a southward shift of the Eemian coastline, thus confirming the results of Dechend (1954) and Dechend & Sindowski (1956).

It is difficult to find precise, or relevant, palaeoenvironmental information for the trace of the fluvial channel(s) during the Weichselian. Based on the geometries of the acoustic reflectors (i.e. westward-dipping orientation of individual reflectors) from F6, an EW-oriented sediment transport direction within the channel was identified, thus suggesting a possible drainage direction towards the Palaeo-Ems (cf. Hepp et al., 2019) (Fig. 7D).

With the onset of the Holocene, large bogs developed in the East Frisian area (Fig. 7E) (Grohne, 1957, 1958; Schlütz et al., 2021). The individual peat beds (F8) contain occasionally sand grains most likely of aeolian origin. Localised brackish-lagoonal (F9) deposits were also noted, and these appear to thicken from W to E, suggesting that the depositional centre was to the E.

## Conclusions

The combination of hydroacoustic methods and sedimentological investigation allowed a series of high-resolution stratigraphic profiles for the western part of the Riffgat channel, at the transition from the tidal inlet to the island of Norderney (Central Wadden Sea, southern North Sea) to be produced. Sediment facies information, derived from eight cores from the WASA project, was correlated

https://doi.org/10.1017/njg.2021.3 Published online by Cambridge University Press

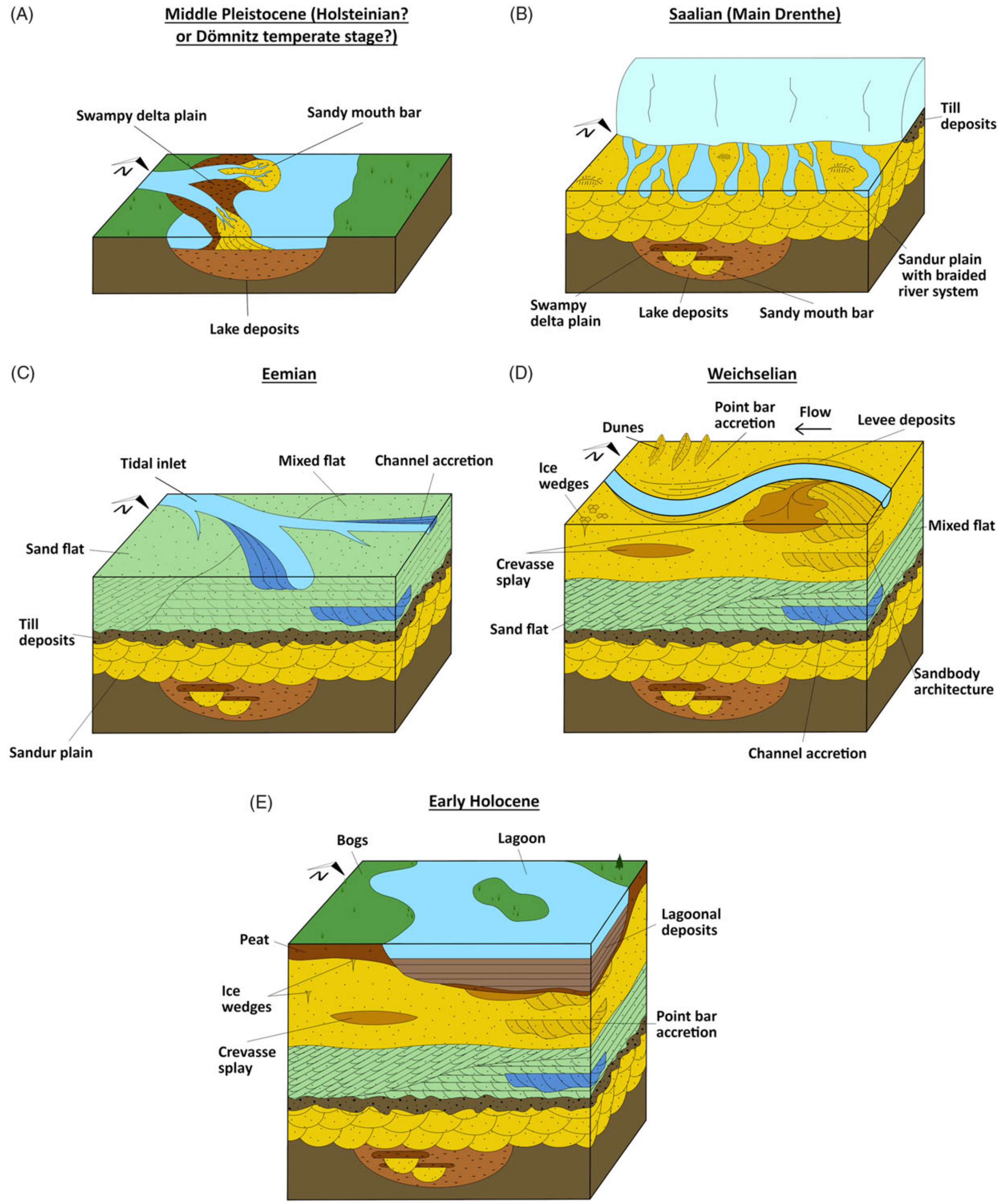


**Fig. 7.** Schematic palaeoenvironmental reconstruction of the Norderney area (figure panels are not to scale; roughly 5 × 5 km). From (A) = oldest to (E) = youngest: (A) Formation of a lacustrine delta in a former Elsterian tunnel valley during the Middle Pleistocene (Holsteinian? or Dömnitz temperate stage). (B) Formation of a sandur plain in front of the glacier, during the Saalian (Main Drenthe). (C) Formation of a transgressional tidal-flat system during the Eemian. (D) Formation of a periglacial meandering river system, with crevasse splays during the Weichselian. (E) Formation of bogs and lagoons during the early Holocene. See Figure 2 for the stratigraphy of Lower Saxony.

with three sub-bottom transects. As a result, acoustic facies could be described and correlated with the lithological and sedimentological facies, resulting in the definition of 12 facies. This integrated approach allowed the palaeoenvironment of a series of Middle Pleistocene lacustrine deposits (Holsteinian? – Dömnitz temperate stage?), the last two interglacials (Eemian-early Holocene), and the last two glacials (Saalian–Weichselian), to be reconstructed, thus illustrating the evolution of the East Frisian area in great detail. Furthermore, eight additional new cores (16 WASA cores in total) and 14 older cores from the LBEG were correlated to generate three short cross-sections at the transition from the tidal inlet (Riffgat channel) to the island of Norderney.

https://doi.org/10.1017/njg.2021.3 Published online by Cambridge University Press

1. The Middle Pleistocene lacustrine deltaic deposits are described for the western part of Norderney for the first time. Sedimentary facies descriptions in combination with the acoustic data suggest that these sediments belong either to the Holsteinian limnic facies or to the Dömnitz temperate stage, which are prominent deposits inside Elsterian tunnel valleys. Such Elsterian tunnel valleys may be present below Norderney.
2. The Saalian moraine (Drenthe Main Till) was documented over large parts of the recent sea floor. As it is an erosionally resistant layer it appears to be a limiting constraint on the vertical development of tidal inlets and the main tidal channels.
3. The core database allowed three new cross-sections across the Riffgat channel and the western head of Norderney to be produced. These cross-sections clearly demonstrate the presence of both Eemian and Middle Pleistocene deposits in the area, in contrast to previously published works.
4. Due to stratigraphic contextualisation, it was possible to recognise a series of Eemian shallow marine deposits between the Saalian moraine (Drenthe Main Till) and the Weichselian fluvial deposits. At the western head of Norderney island, an Eemian mixed tidal-flat system is overlain by Eemian sand tidal-flat deposits.

**Acknowledgements.** This study was performed within the joint research project WASA (The Wadden Sea archive of landscape evolution, climate change and settlement history: exploration – analysis – predictive modelling) funded by the Ministry for Science and Culture of Lower Saxony under ZV 3197. We are grateful to the Wadden Sea National Park administration for fieldwork permission. The EasyCopy company is acknowledged for providing the core-sketching software (EasyCore). We thank the Landesamt für Bergbau, Energie und Geologie (LBEG) for providing the archive core data. Thanks to A. Wurpts, F. Mascioli, T. Kunde (NLWKN), the crews of RV *Burchana* and RV *Senckenberg* and to all of the students who helped during the fieldwork. E. Schindler (Senckenberg Research Institute, Frankfurt) is thanked for determination of the crinoid element found in the fine-gravel fraction. Special thanks to E. Drews for her help in creating the figures. Thanks also to T. Scheidl and L. Schenk-Schlautmann for their support. Furthermore, the authors would like to thank the two anonymous reviewers whose comments greatly helped to improve the manuscript.

**Supplementary material.** Supplementary material is available online at https://doi.org/10.1017/njg.2021.3.

## References


***Bart, P.J. & Anderson, J.B.***, 1997. Seismic record of glacial events affecting the Pacific Margin of the Northwestern Antarctic Peninsula. In: Cooper, A.K., Barker, P.F. & Brancolini, G. (eds): Geology and seismic stratigraphy of the Antarctic Margin. American Geophysical Union (Washington, DC): 75–95.

***Bart, P. & Santis, L.*** de, 2012. Glacial intensification during the Neogene: a review of seismic stratigraphic evidence from the Ross Sea, Antarctica, Continental Shelf. Oceanography **25**: 166–183.

***Behre, K.-E.***, 2004. Coastal development, sea-level change and settlement history during the later Holocene in the Clay District of Lower Saxony (Niedersachsen), northern Germany. Quaternary International **112**: 37–53.

***Behre, K.-E.***, 2007. A new Holocene sea-level curve for the southern North Sea. Boreas **36**: 82–102.

***Behre, K.-E. & Lade, U.***, 1986. Eine Folge von Eem und 4 Weichsel-Interstadialen in Oerel/Niedersachsen und ihr Vegetationsablauf. E&G – Quaternary Science Journal **36**: 11–36.

***Bittmann, F., Bungenstock, F. & Wehrmann, A.***, 2021. Editorial. The Middle Pleistocene to early Holocene subsurface geology of the Nordeney tidal basin. Netherlands Journal of Geosciences, this issue.

***Blott, S.J. & Pye, K.***, 2001. GRADISTAT: a grain size distribution and statistics package for the analysis of unconsolidated sediments. Earth Surface Processes and Landforms **26**: 1237–1248.

***Börner, A., Hrynowiecka, A., Kuznetsov, V., Stachowicz-Rybka, R., Maksimov, F., Grigoriev, V., Niska, M.*** & Moskal-del Hoyo, M., 2015. Palaeoecological investigations and 230Th/U dating of Eemian interglacial peat sequence of Banzin (Mecklenburg-Western Pomerania, NE-Germany). Quaternary International **386**: 122–136.

***Boulton, G.***, 2001. Palaeoglaciology of an ice sheet through a glacial cycle: the European ice sheet through the Weichselian. Quaternary Science Reviews **20**: 591–625.

***BSH – Bundesamt für Seeschifffahrt und Hydrographie***, 2020. Gezeitenkalender – Hoch- und Niedrigwasserzeiten für die Deutsch Bucht und deren Flussgebiete: 135 p.; Hamburg (Bundesamt für Seeschifffahrt und Hydrographie).

***Buckley, F.A.***, 2017. A glaciogenic sequence from the Early Pleistocene of the Central North Sea. Journal of Quaternary Science **32**: 145–168.

***Bungenstock, F., Freund, H. & Bartholomä, A.***, 2021. Holocene relative sea-level data for the East Frisian barrier coast. Netherlands Journal of Geosciences, in revision.

***Bussemer, S.***, 2002. Quartäre Entwicklung und Gliederung der Binnenentwässerungsgebiete auf der Barnimhochfläche (NE-Brandenburg). Greifswalder Geographische Arbeiten **26**: 23–26.

***Capperucci, R.M., Enters, D., Bartholomä, A., Bungenstock, F., Karle, M. & Wehrmann, A.***, 2021. The WASA core catalogue of Late-Quaternary depositional sequences in the Central Wadden Sea, North Germany. Netherlands Journal of Geosciences, this Issue.

***Caspers, G., Merkt, J., Müller, H. & Freund, H.***, 2002. The Eemian interglaciation in northwestern Germany. Quaternary Research **58**: 49–52.

***Collinson, J.D.***, 2009. Alluvial sediments. In: Reading, H.G. (ed.): Sedimentary environments: processes, facies and stratigraphy. Blackwell (Malden, MA): 37–82.

***Coughlan, M., Fleischer, M., Wheeler, A.J., Hepp, D.A., Hebbeln, D. & Mörz, T.***, 2018. A revised stratigraphical framework for the Quaternary deposits of the German North Sea sector: a geological-geotechnical approach. Boreas **47**: 80–105.

***Dechend, W.***, 1950. Das Eem im Raum Nordeney-Hilgenriede. Zeitschrift der Deutschen Gesellschaft **102**: 91–97.

***Dechend, W.***, 1952. Die erdgeschichtliche Entwicklung im Raum Norderney. Zeitschrift der Deutschen Gesellschaft **104**: 429–430.

***Dechend, W.***, 1954. Eustatische und tektonische Einflüsse im Quartär der südlichen Nordseeküste. Geologisches Jahrbuch **68**: 501–516.

***Dechend, W.***, 1958. Marines und brackisches Eem im Raum der Ems-Mündung. Geologisches Jahrbuch **76**: 175–190.

***Dechend, W. & Sindowski, K.-H.***, 1956. Die Gliederung des Quartärs im Raum Krummhörn-Dollart (Ostfriesland) und die geologische Entwicklung der unteren Ems. Geologisches Jahrbuch **71**: 461–490.

***Dury, G.H.***, 1964. Principles of underfit streams. Geological Survey Professional Paper **452A**: 1–67.

***Ehlers, J.***, 1978. Feinkieszählungen nach der niederländischen Methode im Hamburger Raum. Der Geschiebesammler **12**: 47–64.

***Ehlers, J.***, 1979. Fine gravel analyses after the Dutch method as tested out on Ristinge Klint, Denmark. Bulletin of the Geological Society of Denmark **27**: 157–165.

***Ehlers, J.***, 1980. Feinkieszählungen im südlichen Geestgebiet Dithmarschens. Schriften Naturwissenschaftlichen Vereins für Schleswig-Holstein: 37–55.

***Ehlers, J.***, 1990. Reconstructing the dynamics of the North-west European Pleistocene ice sheets. Quaternary Science Reviews **9**: 71–83.

***Ehlers, J. & Linke, G.***, 1989. The origin of deep buried channels of Elsterian age in Northwest Germany. Journal of Quaternary Science **4**: 255–265.

***Ehlers, J., Meyer, K.-D. & Stephan, H.-J.***, 1984. The pre-Weichselian glaciations of north-west Europe. Quaternary Science Reviews **3**: 1–40.

***Ehlers, J., Grube, A., Stephan, H.-J. & Wansa, S.***, 2011. Pleistocene glaciations of North Germany – new results. In: Ehlers, J., Gibbard, P.L. & Hughes, P.D. (eds): Quaternary glaciations – extent and chronology – a closer look. Elsevier (Amsterdam): 149–162.

***Eissmann, L.***, 2002. Quaternary geology of eastern Germany (Saxony, Saxon-Anhalt, South Brandenburg, Thüringia), type area of the Elsterian and Saalian Stages in Europe. Quaternary Science Reviews **21**: 1275–1346.

**Erd, K.**, 1994. Zum Gedenken an Alexander Georg Cepek. 27.11.1929-9.5.1994. Brandenburgische Geowissenschaftliche Beiträge **1**: 127–128.

**Eriş, K.K., Çağatay, M.N., Akçer, S., Gasperini, L. & Mart, Y.**, 2011. Late glacial to Holocene sea-level changes in the Sea of Marmara: new evidence from high-resolution seismics and core studies. Geo-Marine Letters **31**: 1–18.

**Fan, D.**, 2012. Open-coast tidal flats. In: Davis, R.A. & Dalrymple, R.W. (eds): Principles of tidal sedimentology. Springer Netherlands (Dordrecht): 187–229.

**FitzGerald, D.M.**, 2015. Geologic controls on tidal inlets. Journal of Shore and Beach **83**: 59–64.

**Flemming, B.W.**, 2012. Siliciclastic back-barrier tidal flats. In: Davis, R.A. & Dalrymple, R.W. (eds): Principles of tidal sedimentology. Springer Netherlands (Dordrecht): 231–267.

**Flemming, B.W. & Davis, R.A.**, 1994. Holocene evolution, morphodynamics and sedimentology of the Spiekeroog barrier island system (southern North Sea). Senckenbergiana Maritima **24**: 117–155.

**Flemming, B.W., Schubert, H., Hertweck, G. & Müller, K.**, 1992. Bioclastic tidal-channel lag deposits: a genetic model. Senckenbergiana Maritima **22**: 109–129.

**Folk, R.L. & Ward, W.C.**, 1957. Brazos River bar: a study in the significance of grain size parameters. SEPM Journal of Sedimentary Research **27**: 3–26.

**Gelumbauskaitė, L.Ž.**, 2000. Late- and Postglacial palaeogeomorphology on the Klaipėda submarine slope, southeastern Baltic Sea. Baltica **13**: 36–43.

**Geyh, M.A. & Müller, H.**, 2005. Numerical 230Th/U dating and a palynological review of the Holsteinian/Hoxnian Interglacial. Quaternary Science Reviews **24**: 1861–1872.

**Graham, A.G.C., Stoker, M.S., Lonergan, L., Bradwell, T. & Stewart, M.A.**, 2011. The Pleistocene glaciations of the North Sea Basin. In: Ehlers, J., Gibbard, P.L. & Hughes, P.D. (eds): Quaternary glaciations – extent and chronology – a closer look. Elsevier (Amsterdam): 261–278.

**Grant, J.A. & Schreiber, R.**, 1990. Modern swathe sounding and sub-bottom profiling technology for research applications: the Atlas Hydrosweep and Parasound systems. Marine Geophysical Researches **12**: 9–19.

**Grohne, U.**, 1957. Zur Entwicklungsgeschichte des ostfriesischen Küstengebietes auf Grund botanischer Untersuchungen. Probleme der Küstenforschung im südlichen Nordseegebiet **6**: 1–48.

**Grohne, U.**, 1958. Botanische Untersuchung zur geologischen Entwicklung der ostfriesischen Küste von Juist bis Langeoog. Jahresbericht Forschungsstelle Norderney **9**: 31–52.

**Gulliford, A.R., Flint, S.S. & Hodgson, D.M.**, 2017. Crevasse splay processes and deposits in an ancient distributive fluvial system: the lower Beaufort Group, South Africa. Sedimentary Geology **358**: 1–18.

**Hambrey, M.J.** (ed.), 2007. Glacial sedimentary processes and products. IAS/Blackwell Publications (Malden, MA/Oxford): 416 pp.

**Hepp, D.A., Hebbeln, D., Kreiter, S., Keil, H., Bathmann, C., Ehlers, J. & Mörz, T.**, 2012. An east-west-trending Quaternary tunnel valley in the south-eastern North Sea and its seismic-sedimentological interpretation. Journal of Quaternary Science **27**: 844–853.

**Hepp, D.A., Romero, O.E., Mörz, T., de Pol-Holz, R. & Hebbeln, D.**, 2019. How a river submerges into the sea: a geological record of changing a fluvial to a marine paleoenvironment during early Holocene sea level rise. Journal of Quaternary Science **34**: 581–592.

**Hijma, M.P. & Cohen, K.M.**, 2010. Timing and magnitude of the sea-level jump preluding the 8200 yr event. Geology **38**: 275–278.

**Hoselmann, C. & Streif, H.**, 2004. Holocene sea-level rise and its effect on the mass balance of coastal deposits. Quaternary International **112**: 89–103.

**Huijzer, B. & Vandenberghe, J.**, 1998. Climatic reconstruction of the Weichselian Pleniglacial in northwestern and Central Europe. Journal of Quaternary Science **13**: 391–417.

**Huuse, M.**, 2000. Overdeepened Quaternary valleys in the eastern Danish North Sea: morphology and origin. Quaternary Science Reviews **19**: 1233–1253.

**Karle, M., Bungenstock, F. & Wehrmann, A.**, 2021. Holocene coastal landscape development in response to a rising sea level in the Central Wadden Sea coastal region. Netherlands Journal of Geosciences, this issue.

**Kehew, A.E., Piotrowski, J.A. & Jørgensen, F.**, 2012. Tunnel valleys: concepts and controversies – a review. Earth-Science Reviews **113**: 33–58.

**Keilhack, K. & Wildvang, D.**, 1925. Erläuterungen zur Geologischen Karte von Preußen und benachbarten deutschen Landern. Bl. Borkum, Juis-West, Juist-Ost u. Norderney. Preußische Geolgische Landesanstalt (Berlin).

**Kiden, P., Denys, L. & Johnston, P.**, 2002. Late Quaternary sea-level change and isostatic and tectonic land movements along the Belgian-Dutch North Sea coast: geological data and model results. Journal of Quaternary Science **17**: 535–546.

**Knies, J., Kleiber, H.-P., Matthiessen, J., Müller, C. & Nowaczyk, N.**, 2001. Marine ice-rafted debris records constrain maximum extent of Saalian and Weichselian ice-sheets along the northern Eurasian margin. Global and Planetary Change **31**: 45–64.

**Knudsen, K.L.**, 1988. Marine interglacial deposits in the Cuxhaven Area, NW Germany: a comparison of Holsteinian, Eemian and Holocene foraminiferal faunas. E&G – Quaternary Science Journal **38**: 69–77.

**Kraus, M.-J. & Aslan, A.**, 1993. Eocene hydromorphic paleosols: significance for interpreting ancient floodplain processes. SEPM Journal of Sedimentary Research **63**: 453–463.

**Lamb, R.M., Huuse, M. & Stewart, M.**, 2017. Early Quaternary sedimentary processes and palaeoenvironments in the central North Sea. Journal of Quaternary Science **32**: 127–144.

**Lambeck, K., Purcell, A., Funder, S., Kjær, K., Larsen, E. & Möller, P.**, 2006. Constraints on the Late Saalian to early Middle Weichselian ice sheet of Eurasia from field data and rebound modelling. Boreas **35**: 539–575.

**Lang, J., Winsemann, J., Steinmetz, D., Polom, U., Pollok, L., Böhner, U., Serangeli, J., Brandes, C., Hampel, A. & Winghart, S.**, 2012. The Pleistocene of Schöningen, Germany: a complex tunnel valley fill revealed from 3D subsurface modelling and shear wave seismics. Quaternary Science Reviews **39**: 86–105.

**Lang, J., Böhner, U., Polom, U., Serangeli, J. & Winsemann, J.**, 2015. The Middle Pleistocene tunnel valley at Schöningen as a Paleolithic archive. Journal of Human Evolution **89**: 18–26.

**Leduc, G., Schneider, R., Kim, J.-H. & Lohmann, G.**, 2010. Holocene and Eemian sea surface temperature trends as revealed by alkenone and Mg/Ca paleothermometry. Quaternary Science Reviews **29**: 989–1004.

**LGLN**, 2019. Höhenfestpunkte. Produktinformation.

**Lindeque, A., Gohl, K., Henrys, S., Wobbe, F. & Davy, B.**, 2016. Seismic stratigraphy along the Amundsen Sea to Ross Sea continental rise: a cross-regional record of pre-glacial to glacial processes of the West Antarctic margin. Palaeogeography, Palaeoclimatology, Palaeoecology **443**: 183–202.

**Litt, T., Behre, K.-E., Meyer, K.D., Stephan, H.-J. & Wansa, S.**, 2007. Stratigraphische Begriffe für das Quartär des norddeutschen Vereisungsgebietes. E&G – Quaternary Science Journal **56**: 7–65.

**Lutz, R., Kalka, S., Gaedicke, C., Reinhardt, L. & Winsemann, J.**, 2009. Pleistocene tunnel valleys in the German North Sea: spatial distribution and morphology. Zeitschrift der Deutschen Gesellschaft für Geowissenschaften **160**: 225–235.

**Meyer, K.-D.**, 2005. Zur Stratigraphie des Saale-Glazials in Niedersachsen und zu Korrelationsversuchen mit Nachbargebieten. E&G – Quaternary Science Journal **55**: 25–42.

**Murton, D.K. & Murton, J.B.**, 2012. Middle and Late Pleistocene glacial lakes of lowland Britain and the southern North Sea Basin. Quaternary International **260**: 115–142.

**NIBIS® Kartenserver**, 2020a. Boreholes and profiles. Landesamt für Bergbau, Energie und Geologie (LBEG) (Hannover). www.nibis.lbeg.de/cardomap3/?lang=en#.

**NIBIS® Kartenserver**, 2020b. Profiletypes of the coastal Holocene. Landesamt für Bergbau, Energie und Geologie (LBEG) (Hannover). www.nibis.lbeg.de/cardomap3/?lang=en#.

**NIBIS® Kartenserver**, 2020c. Relief of the Holocene basis. Landesamt für Bergbau, Energie und Geologie (LBEG) (Hannover). www.nibis.lbeg.de/cardomap3/?lang=en#.

**Nichols, G.**, 2012. Sedimentology and Stratigraphy. Second Edition. Wiley-Blackwell (Chichester).

**Niedermeyer, R.-O., Verse, G. & Bauerhorst, H.**, 2002. Late Quaternary sedimentation and depositional history of the Greifswalder Bodden (southern Baltic Sea). In: Lampe, R. (ed.): Holocene evolution of the south-western Baltic Coast: geological, archaeological and palaeo-environmental aspects. Greifswalder Geographische Arbeiten 27: 147–153.

**Novak, A., Busetti, M., Zgur, F., Baradello, L., Babich, A., Cova, A., Gordini, E., Romeo, R., Tomini, I., Poglajen, S., Diviacco, P. & Vrabec, M.**, 2017. Thickness of marine Holocene sediment in the Gulf of Trieste (Northern Adriatic Sea). Earth System Science Data Discussions: 1–23.

**Nowel, W.**, 2003. Zur Korrelation der Glazialfolgen im Saale-Komplex Nord- und Mitteldeutschlands am Beispiel des Tagesbaus Jänschwalde in Brandenburg. E&G – Quaternary Science Journal **52**: 47–83.

**Obst, K., Nachtweide, C. & Müller, U.**, 2017. Late Saalian and Weichselian glaciations in the German Baltic Sea documented by Pleistocene successions at the southeastern margin of the Arkona Basin. Boreas **46**: 18–33.

**Ottesen, D., Dowdeswell, J.A. & Bugge, T.**, 2014. Morphology, sedimentary infill and depositional environments of the Early Quaternary North Sea Basin (56°–62°N). Marine and Petroleum Geology **56**: 123–146.

**Phillips, E., Hodgson, D.M. & Emery, A.R.**, 2017. The Quaternary geology of the North Sea basin. Journal of Quaternary Science **32**: 117–126.

**Pierik, H.J. & Cohen, K.M.**, 2020. The use of geological, geomorphological and soil mapping products in palaeolandscape reconstructions for the Netherlands. Netherlands Journal of Geosciences **99**: E9.

**Rappol, M., Haldorsen, S., Jørgensen, P., van der Meer, Jaap J.M. & Stoltenberg, H.M.P.**, 1989. Composition and origin of petrographically-stratified thick till in the northern Netherlands and a Saalian glaciation model for the North Sea Basin. Mededelingen van de Werkgroep voor Tertiaire en Kwartaire Geologie **26**: 31–64.

**Saleh, M. & Rabah, M.**, 2016. Seabed sub-bottom sediment classification using parametric sub-bottom profiler. NRIAG Journal of Astronomy and Geophysics **5**: 87–95.

**Scasso, R.A., Dozo, M.T., Cuitiño, J.I. & Bouza, P.**, 2012. Meandering tidal-fluvial channels and lag concentration of terrestrial vertebrates in the fluvial/tidal transition of an ancient estuary in Patagonia. Latin American Journal of Sedimentology and Basin Analysis **19**: 24–45.

**Scherer, C.M.S., Goldberg, K. & Bardola, T.**, 2015. Facies architecture and sequence stratigraphy of an early post-rift fluvial succession, Aptian Barbalha Formation, Araripe Basin, northeastern Brazil. Sedimentary Geology **322**: 43–62.

**Schlütz, F., Enters, D. & Bittmann, F.**, 2021. From dust till drowned: the Holocene landscape development at Norderney. Netherlands Journal of Geosciences, this issue.

**Schokker, J., Cleveringa, P. & Murray, A.S.**, 2004. Palaeoenvironmental reconstruction and OSL dating of terrestrial Eemian deposits in the southeastern Netherlands. Journal of Quaternary Science **19**: 193–202.

**Serjup, H.P., Haflidason, H., Aarseth, I., King, E., Forsberg, C.F., Long, D. & Rokoengen, K.**, 1994. Late Weichselian glaciation history of the northern North Sea. Boreas **23**: 1–13.

**Shackleton, N.J., Sánchez-Goñi, M.F., Pailler, D. & Lancelot, Y.**, 2003. Marine Isotope Substage 5e and the Eemian Interglacial. Global and Planetary Change **36**: 151–155.

**Sierralta, M., Urban, B., Linke, G. & Frechen, M.**, 2017. Middle Pleistocene interglacial peat deposits from Northern Germany investigated by 230Th/U and palynology: case studies from Wedel and Schöningen. Zeitschrift der Deutschen Gesellschaft für Geowissenschaften **168**: 373–387.

**Sindowski, K.-H.**, 1973. Das ostfriesische Küstengebiet. Inseln, Watten und Marschen: mit 22 Tabellen. Borntraeger (Berlin): 162 pp.

**Smed, P. & Ehlers, J.**, 2002. Steine aus dem Norden. Geschiebe als Zeugen der Eiszeit in Norddeutschland. Borntraeger (Berlin): 194 pp.

**Stackebrandt, W.**, 2009. Die subglazialen Rinnen Norddeutschlands – ein kurzer Überblick. Zeitschrift der Deutschen Gesellschaft für Geowissenschaften **160**: 203–210.

**Stackebrandt, W., Ludwig, A.O. & Ostaficzuk, S.**, 2001. Base of Quaternary deposits of the Baltic Sea depression and adjacent areas (map 2). Neogeodynamica Baltica IGCP-Project-346. Brandenburgische Geowissenschaftliche Beiträge 8: 13–19.

**Stephan, H.-J., Urban, B., Lüttig, G., Menke, B. & Sierralta, M.**, 2012. Palynologische, petrographische und geochronologische Untersuchungen an Ablagerungen der Leck-Warmzeit (spätes Mittelpleistozän) und begleitender Sedimente. Mit 4 Tabellen. In Kommission E. Schweizerbart'sche Verlagsbuchhandlung (Nägele u. Obermiller); Bundesanstalt für Geowissenschaften und Rohstoffe; Landesamt für Bergbau Energie und Geologie (Stuttgart/Hannover/Hannover): 80 pp.

**Streif, H.**, 1990. Das ostfriesische Küstengebiet. Nordsee, Inseln, Watten und Marschen; mit 10 Tabellen. Borntraeger (Berlin): 376 pp.

**Streif, H.**, 1998. Die Geologische Küstenkarte von Niedersachsen 1:25.000 - eine neue Planungsgrundlage für die Küstenregion. Zeitschrift für angewandte Geologie **44**: 183–194.

**Streif, H.**, 2004. Sedimentary record of Pleistocene and Holocene marine inundations along the North Sea coast of Lower Saxony, Germany. Quaternary International **112**: 3–28.

**Streif, H. & Köstner, R.**, 1978. Zur Geologie der deutschen Nordseeküste. Die Küste **32**: 30–49.

**TGL 25 232**, 1971. Fachbereichsstandard Geologie: Analyse des Geschiebestandes quartärer Grundmoränen. Blatt 01-06. Zentrales Geologisches Institut (Berlin).

**TGL 25 232**, 1980. Fachbereichsstandard Geologie: Analyse des Geschiebestandes quartärer Grundmoränen. Blatt 01-05. Zentrales Geologisches Institut (Berlin).

**Turner, C.**, 2000. The Eemian interglacial in the North European plain and adjacent areas. Netherlands Journal of Geosciences **79**: 217–231.

**Unger, K.P., Hübner, F. & Escher, D.**, 1995. Holstein- und Eem-Interglaziale im Bereich des Lausitzer Grenzwalles und die Gliederung der Saalevereisung zwischen Baruther und Lausitzer Urstromtal. E&G – Quaternary Science Journal **45**: 24–31.

**Urban, B.**, 2007. Interglacial pollen records from Schöningen, North Germany. In: The Climate of Past Interglacials. Elsevier (Amsterdam): 417–444.

**Urban, B., Thieme, H. & Elsner, H.**, 1988. Biostratigraphie, quartärgeologische und urgeschichtliche Befunde aus dem Tagebau 'Schöningen', LdKr. Helmstedt. Zeitschrift der Deutschen Gesellschaft für Geowissenschaften **139**: 123–154.

**Urban, B., Sierralta, M. & Frechen, M.**, 2011. New evidence for vegetation development and timing of Upper Middle Pleistocene interglacials in Northern Germany and tentative correlations. Quaternary International **241**: 125–142.

**van Huissteden, J.**, 1990. Tundra rivers of the Last Glacial: sedimentation and geomorphological processes during the Middle Pleniglacial (Eastern Netherlands). Mededelingen Rijks Geologische Dienst **44**: 1–138.

**van Huissteden, J., van der Valk, L. & Vandenberghe, J.**, 1986. Geomorphological evolution of a lowland valley system during the Weichselian. Earth Surface Processes and Landforms **11**: 207–216.

**Vandenberghe, J. & Woo, M.-k.**, 2002. Modern and ancient periglacial river types. Progress in Physical Geography: Earth and Environment **26**: 479–506.

**Vink, A., Steffen, H., Reinhardt, L. & Kaufmann, G.**, 2007. Holocene relative sea-level change, isostatic subsidence and the radial viscosity structure of the mantle of northwest Europe (Belgium, the Netherlands, Germany, southern North Sea). Quaternary Science Reviews **26**: 3249–3275.

**Vos, P.C. & Knol, E.**, 2015. Holocene landscape reconstruction of the Wadden Sea area between Marsdiep and Weser. Netherlands Journal of Geosciences **94**: 157–183.

**Vos, P., van den Meule, M., Weerts, H.J.T. & Bazelmans, J.**, 2020. Atlas of the Holocene Netherlands: landscape and habitation since the last ice age. Amsterdam University Press (Amsterdam): 96 pp.

**Walker, M., Gibbard, P., Head, M.J., Berkelhammer, M., Björck, S., Cheng, H., Cwynar, L.C., Fisher, D., Gkinis, V., Long, A., Lowe, J., Newnham, R., Rasmussen, S.O. & Weiss, H.**, 2019. Formal subdivision of the Holocene Series/Epoch: a summary. Journal of the Geological Society of India **93**: 135–141.

**Wunderlich, J. & Müller, S.**, 2003. High-resolution sub-bottom profiling using parametric acoustics. International Ocean Systems **7**: 6–11.

**Zandstra, J.G.**, 1976. Sedimentpetrographische Untersuchungen des Geschiebelehms von Emmerschans (Drenthe, Niederlande) mit Bemerkungen über eine Typeneinteilung der Saale-Grundmoräne. E&G – Quaternary Science Journal **27**: 30–52.

**Zandstra, J.G.**, 1978. Einführungen in die Feinkiesanalyse. Der Geschiebesammler **12**: 21–38.